journal of the international meteor organization

WGN

33:1
february 2005

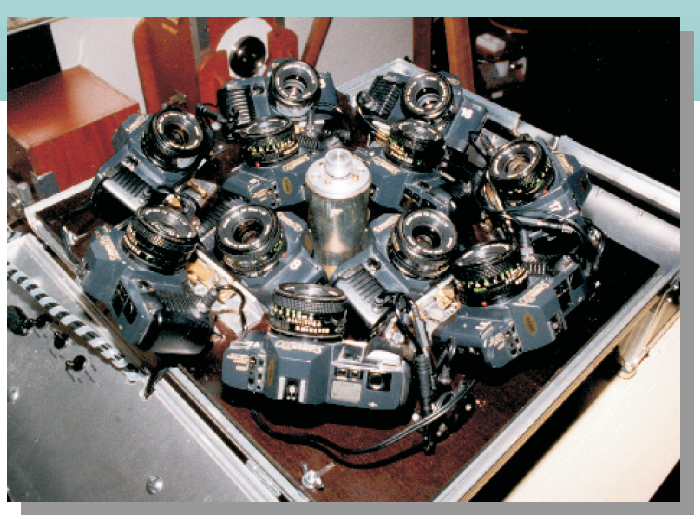

Special Edition on Imaging
Lenses, Spectra, Software
Perseids

ISSN 1016-3115

WGN Vol. 33, No. 1, February 2005, pp. 1 – 32

Administrative

Perseids

Imaging

History

Front cover photo

Part of the 'Hazen' array of meteor cameras used by Robert Haas of the Dutch Meteor Society.

Future covers

Have you an interesting or spectacular meteor photograph that you think would look good on the cover of WGN? If so, please offer it to us. For the moment we can only accept machine-readable forms. More or less any image format will do, though ideally not JPEG as the JPEG compression algorithms lose information. A brief description will also be required: this should say what the photograph shows, when and where it was taken, plus (if possible) technical details such as the camera and exposure. We can be contacted at `wgn@imo.net`, but remember to put 'Meteor' in the subject line to get round the anti-spam filters.

Writing for WGN

This Journal welcomes papers submitted for publication. All papers are reviewed for scientific content, and edited for English and style. Instructions for authors can be found in WGN **31:4**, 124–128, and at `http://www.imo.net/articles/writingforwgn.pdf` .

Cover design

Rainer Arlt

Copyright

Janus

Robert Lunsford [1]

I often look back to the beginnings of my interest in meteors. The first session I can recall was the night of the great Leonid storm in 1966. That previous evening there was a story of the famous Leonid meteor shower on the nightly television news show. Following the program I looked outside only to see totally cloudy skies that evening. Undaunted, I still set my alarm for 01^h00^m and awoke to see clear skies. I bundled up and ventured outside to our driveway. Being youthful and inexperienced, I expected to see a sky full of shooting stars. There were several meteors per minute but it was not enough to overcome the cold and the fact I had to go to school the next morning. Several months later I learned that had I awoke just a few hours later, the sky indeed would have been full of shooting stars. I still tell myself to this day I would never bother viewing on any but the best nights of meteor activity had I witnessed the 1966 at their peak intensity.

For the next decade I viewed the major meteor showers from my backyard and occasionally shared my observations with my only source of astronomy at the time, Sky & Telescope magazine. Evidently someone in the American Meteor Society saw my interest in meteors and sent me a sample copy of their newsletter 'Meteor News'. Wow! A journal devoted just to meteors! I had no idea such a thing existed. I joined the AMS and was one of their most active contributors during the 1980's.

As my horizons expanded I soon learned there were other meteor groups located throughout the world. Each one had their own observing and reporting methodologies and catered to their own local group. Their journals rarely contained data or articles from outsiders. There was even occasional bickering as groups and individuals criticized each other. In 1988, along came an invitation to help form a international meteor group using the same procedures for reporting and analyzing meteor activity. I eagerly became a founding member of the International Meteor Organization as I saw the large potential of such a group. All was not smooth at the start as some groups were still quite nationalistic and saw the I.M.O. as a threat to their existence. Diplomacy was often lacking on both sides and it was not until well into the 1990's that the value of both local groups and a large worldwide organization was accepted by a vast majority of the most active meteor observers. The value of the I.M.O. was clearly demonstrated during the recent Leonid revival when timely articles and results were produced and published. It was also a good opportunity for observers of all backgrounds and nationalities to observe together and enjoy the splendor of meteor-streaked skies.

The I.M.O. is run by a small group of dedicated people who volunteer their spare time. While far from perfect, we still do an admirable job for such a far-flung group. I look forward to the future of the I.M.O. and feel very positive it can continue to contribute at a high level to our knowledge of meteor science. We should appreciate all, whether on a local or global level, who contribute their time and efforts to help share the wonders of the heavens above.

Janus *was a Roman god with two faces, one looking to the past and one to the future, called upon at the beginning of any enterprise. Today he is often a symbol of re-appraisal at the start of the year.*

Editorial

Chris Trayner

This issue is a Special Edition on Imaging. The intention is to gather together a range of papers on a specialist topic of interest to meteor observers. Most of the ones here have been specially written at my request for this issue; we owe the authors a debt of gratitude for their efforts.

If you feel this Special Edition is a success, please feel free to suggest themes for others. Problems (principally, peoples' time) have prevented this Special Edition appearing last Summer as intended. In the light of experience, I would now say that nearly a year's lead time is needed for such an enterprise, to allow time for the authors to write specially commissioned papers despite all their other commitments.

The idea for this Special Edition came from discussions at the International Meteor Conference in 2003. Like any good conference, IMC is a place to talk to like-minded people. New ideas often spring from discussions, along with a renewed sense of enthusiasm for the subject. The conference this September will be in Belgium; details can be found on page 3. I look forward to seeing you there.

[1] *161 Vance Street, Chula Vista, CA 91910-4828, USA. Email:* lunro.imo.usa@cox.net

Letter — Luminosity function of sporadic video meteors

Milos Weber [1]

I tried to derive the luminosity function of sporadic video meteors and the population index from the set of 372 sporadic meteors included in (Koten et al., 2003). The magnitudes of meteors included in this catalogue are absolute. The luminosity function was constructed by the method of cumulative counts. The resulting function (Figure 1) is almost exactly linear in the interval of $M = 0.5$ to 3.0 with the slope $k = 0.475108$ i.e. $r = 2.99$. All corrections are included during the reduction to absolute magnitude.

For comparison we cite the most recently published value of $r = 2.95$ for visual sporadic meteors (Rendtel, 2004, summarised in Anon, 2004, p.4). This r value was derived using all correction factors according to the IMO method, from a set of 301 499 sporadic meteors.

These comments are restricted to the derived luminosity function and the population index; the theoretical consequences are left to the specialists.

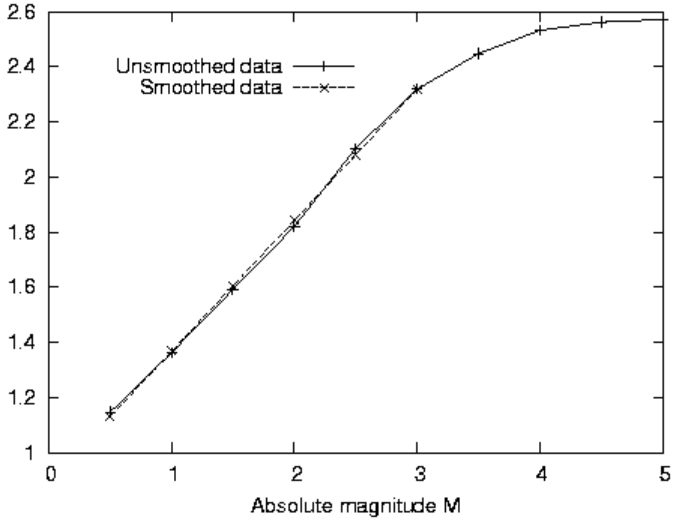

	Unsmoothed		Smoothed	
M	Σn	$\log(\Sigma n)$	Σn	$\log(\Sigma n)$
5.0	372	2.570543	1851.3	3.267488367
4.5	364	2.561101	1071.4	3.029934554
4.0	340	2.531479	620.0	2.792380740
3.5	280	2.447158	358.8	2.554826926
3.0	208	2.318063	207.6	2.317273113
2.5	127	2.103804	120.1	2.079719299
2.0	66	1.819544	69.5	1.842165485
1.5	39	1.591065	40.2	1.604611672
1.0	23	1.361728	23.3	1.367057858
0.5	14	1.146128	13.5	1.129504044

$k = 0.475107627$; $q = 0.891950$
$r = 10^k = 2.99$

Figure 1 – Logs of sums of meteor counts *versus* absolute magnitude M. The shorter curve, running up to M=3, is based on smoothed sums. Right: the data used for the graph.

References

Anon (2004). "Details of Proc. IMC 2003". *WGN*, **32:1**, 4.

Koten P., Spurny P., Borovicka J., and Stork R. (2003). "Catalogues of video meteor orbits – Part 1, years 1998–2001". `http://www.asu.cas.cz/meteor/catalogues`.

Rendtel J. (2004). "The population index of sporadix meteors". In *Proc. IMC 2003*, pages 114–122.

Correction — An α-Capricornid meteor spectrum, Borovička and Weber, WGN 24:1–2, 30–32

Figure 1 of this paper (Borovička & Weber, 1996) was rotated clockwise during editing, but the caption was not modified to match. The relevant part of the caption should read 'The meteor moved from top right to bottom left. Wavelengths increase from right to left.'

References

Borovička J. and Weber M. (1996). "An α-Capricornid meteor spectrum". *WGN*, **24:1–2**, 30–32.

[1] *Verdunská 19, Praha 6, 160 00, Czech Republic.*

International Meteor Conference 2005 September 15–18, Oostmalle, Belgium

The IMC 2005 Committee

The first time

For the first time since the foundation of IMO, the International Meteor Conference will be held in Belgium, on September 15–18, 2005. Oostmalle is a Belgian village located 30 km northeast of the beautiful city of Antwerp, second largest city of Belgium, fourth largest port in the world, and the world capital of diamonds. Urania, the Public Observatory of Antwerp, has maintained regular contacts with IMO since 1988. Actually, Urania is IMO's official seat, and its meteor section is very proud to organize this IMC.

Go Belgian

The conference center 'Provinciaal Vormingscentrum' lies in a green area, and offers accommodation for 100 people or more (rooms for 1 to 6 persons). There is one big lecture hall and some smaller well-equipped rooms with Internet access. The evenings can be spent in the two cosy bars we have at our disposal. Beer lovers can taste a selection of the finest Belgian beers there.

The weather

The temperature is typically around 15–20 degrees Celsius (60-70 degrees Fahrenheit) in September.

Currency

The official currency in Belgium is the Euro. Foreign currency can be exchanged in banks and exchange offices.

The excursion

A traditional part of the program is the excursion, which will lead us to the nice and small characteristic city of Lier, famous for its beguinage and the 'Zimmertoren'. Even Albert Einstein was impressed by this old tower in which Louis Zimmer built a whole range of high-quality astronomical clocks in the 1930s.

Participation fee

If you wish to register, please fill out the registration form on the next page or register online at the IMC 2005 website (see below). The participation fee for the IMC 2005 is €120 for people who register before July 1st and €130 for those who register later. This fee includes lodging, meals, excursion and the Proceedings. Either a prepayment of €60 or the total amount should be sent to IMO treasurer Ina Rendtel (details inside back cover and IMC 2005 website).

Visas and invitations

We will gladly send official invitations to people who need these to get a visa, provided that they inform us about this in due time. You can find out on the IMC website whether visa are required for citizens of your country.

Radio meteor school 2005

We proudly present the 'Radio Meteor School 2005', a five-day tutorial (Oostmalle, September 10 till 14) in which Prof. Dr. Oleg Belkovich, Russian eminence grise in meteor astronomy, will lecture on the physical and mathematical theory of radio meteor observations. We stress the fact that this is not an easy course, and it will be helpful only to devoted radio observers highly skilled in mathematics and willing to get the utmost data out of their observations. For these people, it is very worthwhile to arrive in Belgium five days before the IMC to participate in the Radio Meteor School. The additional price will be around €150, and should only be paid upon arrival. However, you must register for this school before July 1st. Contact the organizers in order to register.

Contact information

For more information, check the IMC 2005 website at http://www.imo.net/imc2005 or contact the organizers by e-mail at imc2005@imo.net. You can also write to us: IMC 2005 — Jan Verbert, Public Observatory Urania, Jozef Mattheessensstraat 60, B-2540 Hove, Belgium.

International Meteor Conference Oostmalle, Belgium, September 15–18, 2005
Registration form

Each individual participant should fill out a form and return it to IMC 2005 — Jan Verbert, Public Observatory Urania, Jozef Mattheessensstraat 60, B-2540 Hove, Belgium, as soon as possible. Your registration will be guaranteed only after Ina Rendtel has received the minimum pre-payment of €60. If you wish to participate, but cannot yet decide, simply return this form with the proper option checked to stay on the mailing list for further circulars.

Name: _____ Date of birth (YYYY-MM-DD): _____

Address: _____

_____

_____

Phone: _____ Fax: _____ E-mail: _____

- I wish to register for the IMC 2005 from September 15 to 18.
- I intend to participate, cannot yet register, but wish to stay on the mailing list.
- I intend to travel by _____, together with _____
- I need travel information from _____ to Oostmalle.
- I wish to stay in Belgium before and/or after the IMC and would like additional information.
- Vegetarian.

T-shirt: Size (S-M-L-XL): _____ Gender: _____

For participants wishing to contribute to the program:
Lecture: _____ Duration: _____ minutes

Workshop or discussion: _____

Poster presentation: _____ Space: _____ m^2

Required equipment: _____

Comments:

Either the entire fee of €120 or a pre-payment of €60 should be sent to IMO treasurer Ina Rendtel. Follow the payment instructions inside the back cover or on the IMC 2005 website `http://wwww.imo.net/imc2005` . Participants making a pre-payment only have to pay the remaining €60 in cash upon arrival in Oostmalle. The registration fee increases to €130 for participants registering after July 1st.

The following payment options are available.

- **International bank transfer** payments should be made to Ina Rendtel, Mehlbeerenweg 5, D-14469 Potsdam, Germany, BIC bank code: PBNKDEFF, IBAN code: DE86 1001 0010 0547 2341 07. When paying, always state BIC bank code and IBAN code together. Always contact your local bank to verify charges for international transfers.
- **German postal giro** Pay in euros to the German postal giro account 547234-107 of Ina Rendtel, Postbank Berlin. Bank code 100 100 10. The bank code and 'Postbank Berlin' should be mentioned together with account number.

Perseids

The 2004 Perseid fireball night over Spain

Josep Maria Trigo-Rodríguez [1], *Alberto Castro-Tirado* [2], *Martin Jelínek* [2], *Antonio de Ugarte Postigo* [2], *Jordi Llorca* [3], *Tomás J. Mateo Sanguino* [4], *Albert Sánchez Caso* [5], *Francisco Ocaña* [6], *Carles Pineda* [7], *Sebastià Torrell* [8], *Ángela del Castillo* [9], *Joan M. Bullón Lahuerta* [9], *Antonio Bernal González* [10], *Luís Lahuerta* [11], *Salvador Lahuerta* [11], *José Patiño* [11], *Feliciano Villares* [11], *Juan Pastor Erades* [12], *Cándido Gómez* [13], *Fernando García Marín* [14], *and José Carlos Millán López* [15]

An impressive display of Perseid fireballs occurred during the night of 2004 August 11–12. We include a preliminary report of the observed activity together with an example of a high-accuracy trajectory and orbital data on one $m = -8$ Perseid fireball recorded from two amateur stations collaborating in the Spanish Meteor Network (SPMN).

Received 2005 January 19

1 Introduction

We report accurate data on a bright fireball recorded by several amateur stations participating in the 2004 Perseid Campaign organized by the Spanish Meteor Network (SPMN). An impressive display of bright Perseid fireballs occurred during the night of 2004 August 11–12. The fireball studied here is only one example among several remarkable events that are already being analyzed by our team, including several beautiful 'Earth-grazing' fireballs (Figure 1). Although this background of bright meteors was present before and after the outburst, most of these large meteoroids encountered the Earth at $02^{\rm h}$ UT corresponding to $\lambda_{\odot} = 139\,^{\circ}65$, a few hours after the predicted time for the interception of the 2004 Perseid one-revolution outburst perturbed by Jupiter (Lyytinen & Van Flandern, 2004).

The professional part of our network was composed of two all-sky CCD cameras located in Huelva and Málaga belonging to the Instituto de Astrofísica de Andalucía (IAA-CSIC) that started continuous double-station fireball coverage inside the Spanish Fireball Network (Trigo-Rodríguez et al., 2005b). Two additional video stations were operated by members of the IAA in La Sagra and Sierra Nevada (Granada) recording tens of fireballs including a −11 Perseid fireball on August 12, at $02^{\rm h}20^{\rm m}50^{\rm s}$ UT with a persistent train lasting for more than 5 minutes in the sky. An additional meteor spectroscopy campaign was performed using CCDST8E cameras and $f/2.8$, $f = 50$ mm lenses. In fact, an excellent Perseid spectrum with a resolution of ∼0.3 nm/pixel was obtained (Trigo-Rodríguez et al., 2005a). The complete results of this campaign are beyond the scope of this preliminary paper where we wish to give an example of the coverage provided by additional stations operated by amateur astronomers. In a new record of participation, thirteen amateur stations distributed along the east and south of Spain were supporting the work made from four professional stations. We present here the trajectory and orbital data for an impressive Perseid fireball that is one of the brightest of this stream detected by our network in double station since one of $M = -9$ was registered during the magnificent 1993

Figure 1 – All-sky CCD image of a −6 absolute magnitude 'Earth Grazing' Perseid fireball recorded from the station of La Mayora (BOOTES–2) on 2004 August 11 between $21^{\rm h}48^{\rm m}$ and $21^{\rm h}50^{\rm m}30^{\rm s}$ UT.

[1]Astrobiology Center, Institute of Geophysics and Planetary Physics, UCLA, CA 90095-1567, USA. Email: jtrigor@ucla.edu
[2]Instituto de Astrofísica de Andalucía (IAA-CSIC), PO Box 3004, 18080 Granada, Spain.
[3]Institut d'Estudis Espacials de Catalunya, Edifici Nexus, Gran Capità 2–4, 08034 Barcelona, Spain.
[4]Dpto. Ingeniería Electrónica, Sistemas Informáticos y Automática, Universidad de Huelva, Spain.
[5]Gualba Observatory, MPC 442, Barcelona, Spain.
[6]Agrupación Astronómica de Madrid (AAM)
[7]Observatori de l'Alt Empordà, MPC J91, Girona.
[8]Grup d'Estudis Astronòmics (GEA).
[9]Cosmofísica
[10]Asociación Astronómica de Castelldefels (AAC)
[11]Grupo de Estudio, Observación y Divulgación de la astronomía (GEODA)
[12]Agrupació Astronòmica de Sabadell
[13]Agrupación Astronómica Albireo, Sevilla
[14]Agrupación Astronómica Actuel, Teruel
[15]Asociación Astronómica Hubble, Jaén

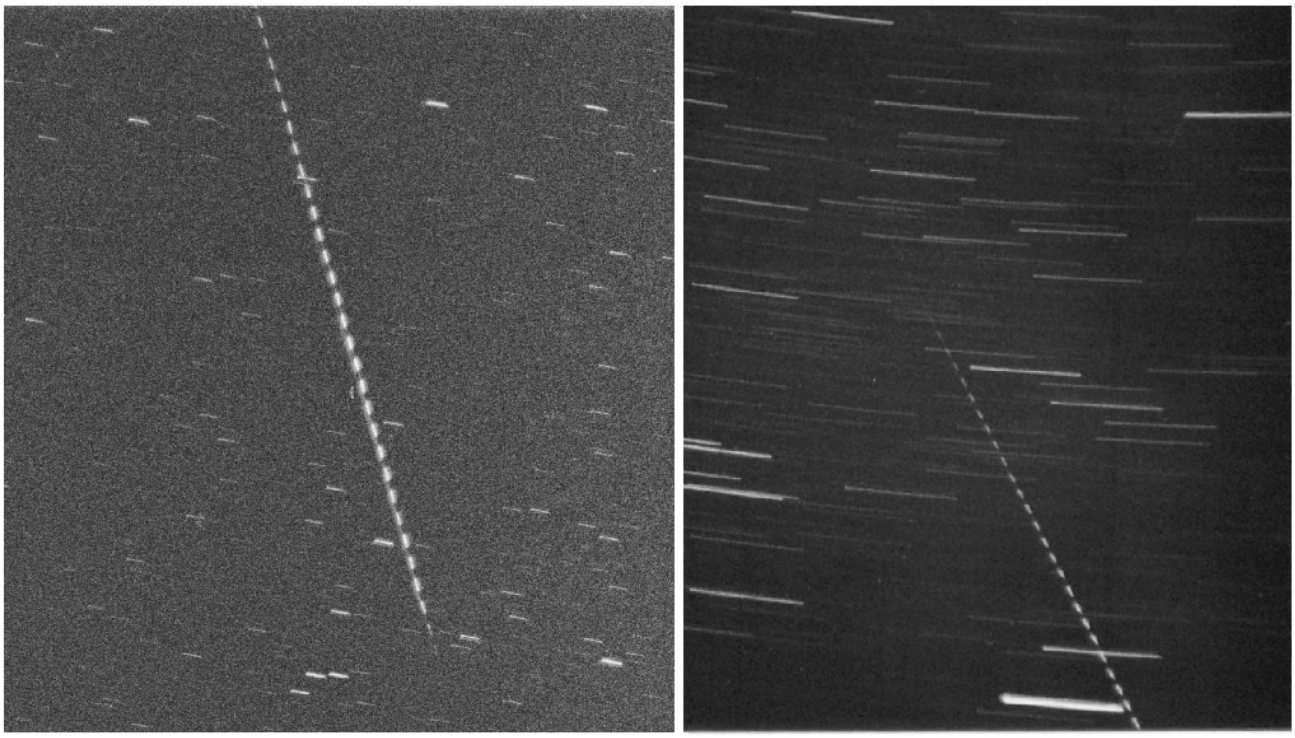

Figure 2 – The SPMN010804 fireball photographed on the left image from Bonilla (Cuenca) and on the right from Titaigües (València). The fireball's movement was from the bottom right to the top left in both images.

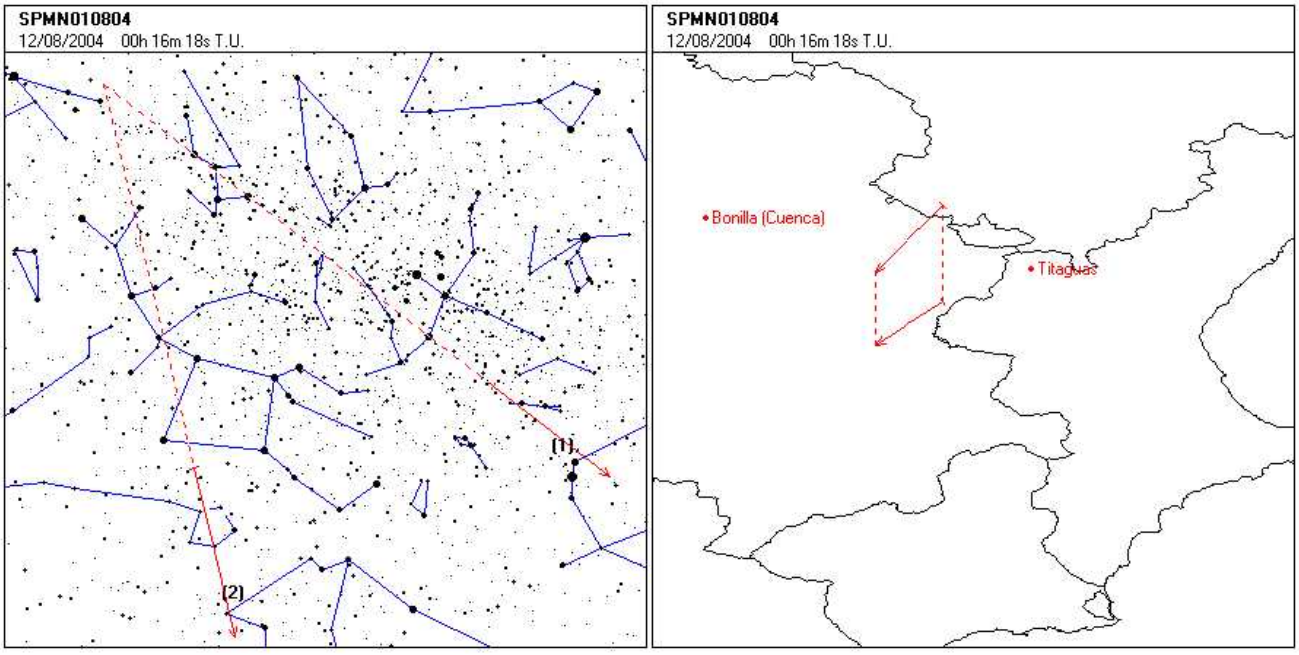

Figure 3 – The projection on the sky of the apparent fireball path (left) from Titaigües (1) and Bonilla (2). The true atmospheric trajectory is projected on the ground (right).

Perseid display. The atmospheric trajectory was obtained, but unfortunately there were no velocity data to compute the heliocentric orbit (Trigo-Rodríguez, 1997).

In order to organize the amateur effort, we program the observations using our software photographic centers. We send electronic mail to the participants, who receive a stellar chart and information about the center of field at which to point their camera according to their station coordinates and the required geometry to maximize detection probability and velocity accuracy. In this way we can optimize observations made from different techniques (photography, CCD and video) and also maximize the atmospheric coverage (Trigo-Rodríguez et al, 2004).

2 The SPMN010804 fireball

One bright fireball recorded by our network during the 2004 Perseid campaign was seen and recorded on August 12 at $00^h16^m18^s$ UT by several amateur astronomers. The astrometric measurements and determination of the trajectory were made using the Network software (Trigo-Rodríguez et al, 2002, 2004). The fireball traveled 39.5 km in 0.65 seconds and was registered by two SPMN amateur stations participating in the Perseid Campaign (Figures 2 and 3). Both stations were equipped with batteries of cameras built in collaboration with Hans Betlem (DMS) (Trigo-Rodríguez et al, 2000). Both batteries were equipped with cameras with 50 mm lenses and four-arm rotating shutters having a frequency of 12.5 Hz and consequently producing 50 breaks/second. The fireball shows up in the common center between stations, and trajectory and orbit are very reliable (Table 1). We give in this Table a rough estimation of the 'instantaneous' photometric mass, i.e. that contributing to the light in different parts of the trail using the measured absolute magnitude. It was estimated following the equation obtained by Verniani (1973). The fireball reached its maximum luminosity over the region of Iniesta (Cuenca) which consequently gave the name to this fireball. The heliocentric orbit plotted in Figure 4 was computed using the program MORB (Ceplecha et al, 2000).

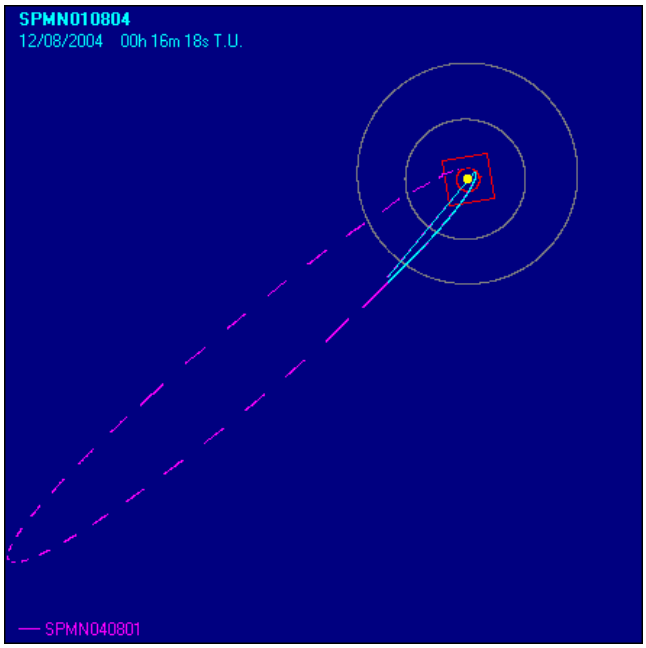

Figure 4 – Heliocentric orbit of SPMN010804. For comparison the orbits of the Earth, Jupiter and Saturn are shown, looking down on the Solar System from the south pole. The square in the centre represents the ecliptic plane. The dashed part of the meteoroid orbit is below that plane, the solid part above it. The straight line pointing down to the left from the Sun indicates the Vernal Equinox.

Acknowledgements

The Ondřejov Observatory team kindly provided the MORB software used to determine accurate meteoroid orbits. We also thank Hans Betlem (Dutch Meteor Society) for helping us build batteries of cameras allowing reliable amateur participation in our network. Finally, we are grateful to all amateur astronomers who participate in SPMN campaigns.

References

Ceplecha Z., Spurný P., and Borovička J. (2000). *MORB software to determine meteoroid orbits.* Ondřejov Observatory, Czech Republic.

Lyytinen E. and Van Flandern T. (2004). "Perseid one-revolution outburst in 2004". *WGN*, **32:2**, 51–53.

Trigo-Rodríguez J. (1997). "Impressive Perseid fireball over Spain". *WGN*, **25:4**, 187–189.

Trigo-Rodríguez J., Castro-Tirado A., and Llorca J. (2005a). "Evidence for hydrated 109P/Swift-Tuttle meteoroids from meteor spectroscopy". In *36th Lunar & Planetary Conference*. Abstract.

Trigo-Rodríguez J., Castro-Tirado A., Llorca J., Fabregat J., Martínez V. J., Reglero V., Jelínek M., Kubánek P., Mateo T., and de Ugarte Postigo A. (2005b). "The development of the Spanish Fireball Network using a new all-sky CCD system". *Earth, Moon & Planets*. Submitted.

Trigo-Rodríguez J., Fabregat J., Llorca J., Castro-Tirado A. J., del Castillo A., de Ugarte A., López A. E., Villares F., and Ruiz-Garrido J. (2000). "Spanish Fireball Network: current status and recent orbit data". *WGN*, **29:4**, 139–144.

Trigo-Rodríguez J., Llorca J., and Fabregat J. (2002). "On the origin of the 1999 Leonid storm as deduced from photographic observations". *Earth, Moon & Planets*, **91**, 107–119.

Trigo-Rodríguez J., Llorca J., Lyytinen E., Ortiz J., Sánchez Caso A., Pineda C., and Torrell S. (2004). "2002 Leonid storm fluxes and related orbital elements". *Icarus*, **171**, 219–228.

Verniani F. (1973). "An analysis of the physical parameters of 5759 faint radio meteors". *Journal of Geophysical Research*, **78**, 8429–8462.

Table 1 – The basic data of SPMN040801.

SPMN010804 'Iniesta'			
2004 August 12, T = $00^h16^m18^s \pm 1^s$ UT			
Atmospheric trajectory data			
	Beginning	Max. light	Terminal
Velocity (km/s)	60.7 ± 0.2	60.5 ± 0.2	59.7 ± 0.2
Height (km)	123.85 ± 0.07	104.34 ± 0.07	86.13 ± 0.06
Longitude (°W)	1.479 ± 0.001	1.677 ± 0.001	1.862 ± 0.001
Latitude (°N)	39.651 ± 0.001	39.477 ± 0.001	39.314 ± 0.001
Photometric mass (kg)	$8 \cdot 10^{-9}$	$9.8 \cdot 10^{-3}$	$2 \cdot 10^{-8}$
Absolute magnitude	6	-8	5
Total length (km)		39.5	
Slope (°)		72.7 ± 0.1	
Duration (s)		0.65	
SPMN stations:	Titaigües (Valencia) and Bonilla (Cuenca)		
Radiant data (J2000.0)			
	Observed	Geocentric	Heliocentric
Right ascension (°)	44.90 ± 0.04	45.61 ± 0.04	-
Declination (°)	57.55 ± 0.04	57.67 ± 0.04	-
Ecliptical longitude (°)	-	-	79.44 ± 0.09
Ecliptical latitude (°)	-	-	63.37 ± 0.06
Initial velocity (km/s)	60.7 ± 0.1	59.5 ± 0.1	41.47 ± 0.09

Orbital data (J2000.0)

a (AU)	29 ± 7	ω (°)	153.75 ± 0.13
e	0.966 ± 0.008	Ω (°)	139.57728 ± 0.00001
q (AU)	0.9620 ± 0.0003	i (°)	113.51 ± 0.07
Q (AU)	56 ± 14		

Imaging

Fisheye lenses

Felix Bettonvil [1]

In meteor astronomy the fisheye lens is well known, in particular in the field of fireball imaging. In this paper all relevant characteristics of the fisheye lens are described and compared with their alternatives.

Received 2005 March 6

1 Introduction

A lens has two parameters which are important for meteor observations, aperture and focal length. The aperture determines the amount of light which enters the camera, the focal length describes the field of view (FoV). In this paper we concentrate on the imaging of fireballs. For them the amount of light is never a limiting factor, i.e. the aperture never plays an important role. The field of view will, however, because fireballs are rare and can appear in any part of the sky. The most extreme lens type in terms of field of view is the fisheye lens. Usually these cover 180° or even more.

Fisheye lenses differ in their appearance from other lenses. Although apertures are small they do have a big front lens, often strongly curved, which gives them their characteristic look. In several designs the front lens is even bigger than the lens body, giving them a mushroom-like shape.

Almost all camera manufacturers offer fisheye lenses. There exist basically two types, having different focal lengths. In 35 mm photography the longer one has a focal length in the range of 16 mm and fills the complete film area of 24×36 mm with the diagonal of the frame (measuring 43 mm) covering 180°. These are known as full frame fisheye lenses. An example is shown in Figure 2 right. The shorter one has a focal length of around 8 mm (Nikon offers a 8 mm one, Figure 2 middle, Canon a 7.5 mm) and measures 180° over the short side of the film. The image is a circle and the corners of the film are unexposed. 8 mm fisheye lenses are called circular fisheye lenses. As against the full frame fisheye lens, they do image the whole hemisphere. It is clear, however, that the image scale is smaller when compared to a full frame lens. In Figure 1 the image scale of both lenses is illustrated. In meteor photography both types are used. The 8 mm is nevertheless not the shortest fisheye lens on the market. Nikon offers a 6 mm type with a field size of 220° (Figure 2 top left). For meteor work these are of course of no use.

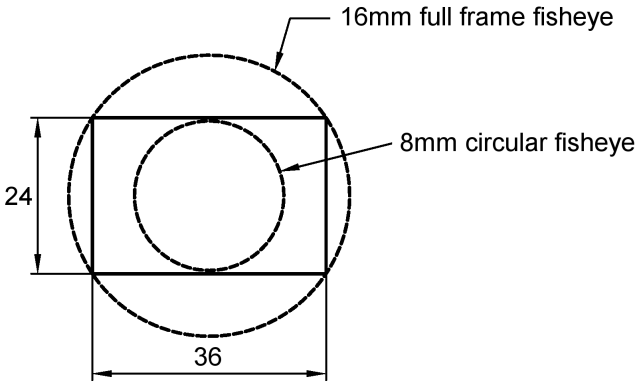

Figure 1 – Comparison of image of a full frame and circular fisheye on 35 mm film. The first exposes the whole film and measures 180° over the diagonal; the latter illuminates a circle with diameter 180°.

2 Fisheyes, wide-angle lenses, reflecting all sky mirrors

Not only 35 mm fisheye lenses exist. For the medium format (58×58 mm) one can buy 16 and 30 mm lenses, comparable with the 8 and 16 mm in 35 mm photography. The 30 mm is a full frame fisheye but inventive hobbyists can turn it into a circular one by making their own camera body housing 4×5″ (i.e. quarter-plate) film (Rendtel, 1993). The longest focal length fisheye is a f=37 mm Mamiya (Figure 2 bottom). Fisheye lenses for digital photography and video (Coastal Optical Systems Inc., 2005) are also being offered.

Fisheye lenses are not identical to wide angle lenses. The latter are corrected for distortion, resulting in a more natural image, see Section 5. This makes them even more expensive and the field of view is smaller compared to fisheye lenses, e.g. a 15 mm super wide angle lens has a field of view of 'only' 110°.

There are also so-called fisheye converters: optics mounted on front of a standard or wide angle lens, which reduce the focal length and increase the field of view. These however are not real fisheye lenses. Despite the attractive price the quality is in general poor, as they suffer strongly from vignetting and often do not reach the full 180°, particularly when the front lens is flat. Converters are not generally designed for a particular lens but for use on a wide range of lenses.

Despite the fact that the fisheye lens is the only one covering the full 180°, there is an alternative for all-sky cameras which is extensively used in fireball patrol work too. This consists of a conventional camera body with standard or small tele-lens, facing a big convex mirror. The camera is then visible in the center of the image, but it easily generates a field of view of 180° and is a cheaper alternative to the more expensive fisheye lenses. Gasden (1978) described a reflecting all-sky camera based on two convex mirrors. Depending on the focal ratio of the camera lens, fast f-ratios are

[1]Astronomical Institute, Utrecht University, PO Box 80000, 3508 TA Utrecht, The Netherlands.
Email: F.C.M.Bettonvil@astro.uu.nl

Figure 2 – A few examples of fisheye lenses: Top left: Nikkor 6 mm $f/2.8$ circular fisheye (field of view 220°). Middle: Nikkor 8 mm $f/2.8$ circular fisheye. Right: Nikkor 16 mm $f/2.8$ full frame fisheye. Bottom: Mamiya 37 mm $f/4.5$ full frame fisheye lens.

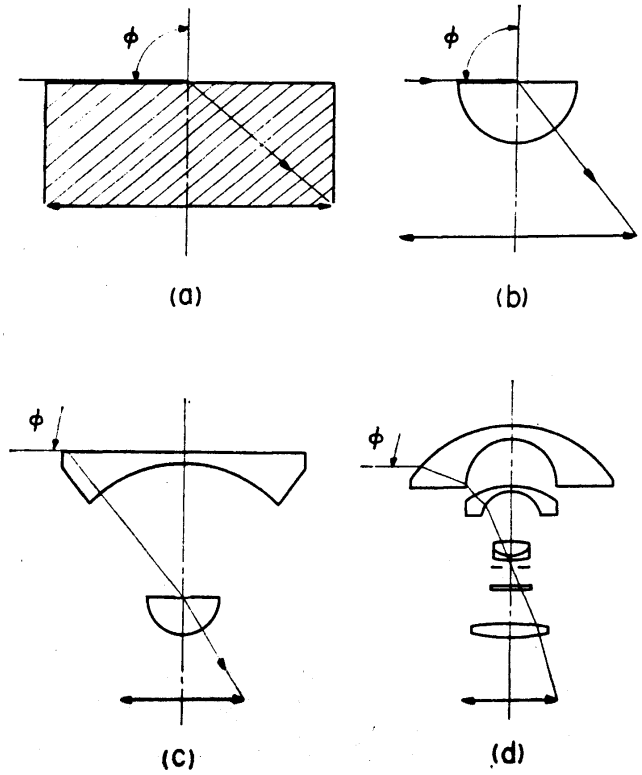

Figure 3 – Development of the fisheye lens: (a) Wood's pinhole camera filled with water; (b) plano-convex lens of Bond; (c) improvement by Hill with negative meniscus lens, which can be seen as the prototype of the modern fisheye (d).

feasible; however even for moderate focal ratios the accuracy cannot be compared with that of a fisheye lens, even when a convex mirror is used of optical quality, due to field curvature caused by the mirror.

3 History of the fisheye lens

The idea behind the fisheye lens is approximately a century old. The name 'fish eye' does not have its origin from the shape of the lens, but from the fact that a fish can see above the water and has there a much larger field of view due to the refraction difference between water and air. In 1919 Wood filled a pinhole camera with water (!), Figure 3a, and was the first in history to make a fisheye exposure. Note that this was about a century after the discovery of the camera obscura as a photographic instrument (1826). In 1922, Bond made other fisheye exposures but he replaced the liquid with a plano-convex spherical lens. Wood's camera did not collect a lot of light; Bond's did, however. The biggest problem with Bond's lens was the enormous field curvature, influencing the sharpness over the field. In 1926 Hill improved the design by adding a big negative meniscus lens in front of Wood's plano-convex lens, and this lens can be seen as the beginning of the modern fisheye design (Miyamoto, 1964).

The fisheye lens is used nowadays in art and architecture, but the real reason for the development of the modern fisheye lens was purely scientific. The lens was useful for photographing the whole sky, for measuring the relative percentage of clouds, study of the viewing angle in cars and air traffic control towers, and inspection of small spaces, tubes and corridors. For inspection of tubes, the area at the edge of a 180° fisheye lens is the most interesting zone, and this was the reason for the development of the 220° type. Despite the fact that Naumann published a complete construction drawing in 1954, it was not until 1965 that the first fisheye lenses became commercial available. The big pioneer was Nikon; for different applications Nikon alone developed six different types, of which four are of a different design (Vorst, 1978).

4 Optical characteristics

As already mentioned, the big negative meniscus lens at the front is the element giving the fisheye lens its unique shape. This element generates the enormous viewing angle, while the second positive lens forms the image on the film plane. In modern fisheye lenses two lens groups together ensure that the distance between the last lens and the image plane (called BFL, back focal length) is larger than the focal length. This is necessary to be able to lift the mirror in a SLR camera. This optical design is called **retrofocus** or inverted telelens design (Laikin, 2001). To create enough BFL a heavily curved front lens is essential. Some of the older fisheye lenses do not use the retrofocus principles, and therefore the mirror has to be lifted before the lens can be attached to the camera body.

Designing a fisheye requires different design strategies from those used for other photo-lenses: in conventional photo-optics the design process starts with objects at infinity. After correction for all aberrations, in the last stage the object distance is varied and all parameters are changed slightly to reach optimum performance. Because of the enormous depth of field of a fisheye lens this technique does not work. Fisheyes suffer from the fact that the position of the pupil starts to shift forwards with increasing viewing angle. The extreme viewing angle causes lateral color too, which is responsible for a color-dependent image scale at the edge. This is difficult to correct.

5 Distortion

Fisheyes have a hemispherical view. In order to image the complete hemisphere on a flat image plane it is inevitable that there is distortion. For wide angle and extreme wide angle lenses this distortion is seen as an aberration and one of the design criteria is to minimize it. Distortion does not affect the sharpness of the image but makes it look unnatural.

Every lens has its projection formula which describes the relation between the entrance angle and the location on the image. For a conventional (**rectilinear**) photographic lens without distortion the projection formula is:

$$r = f \tan(\theta) \tag{1}$$

where θ is the entrance angle, measured from the optical axis; f is the focal length and r is the distance at the image plane measured from the optical axis. It can

easily be seen that this formula could never work for a fisheye where $\theta = 90°$ (on the horizon) would require the image plane to have infinite size.

Because the distortion is not a fixed parameter and can be chosen, more than one projection formula exists. The following two are most frequently used:

$$r = f\theta \tag{2}$$

$$r = 2f\sin(\theta/2) \tag{3}$$

The first projection formula is called **equidistant projection** (sometimes called orthographic projection, though this is wrong as we will see later). This one is desirable when measuring zenith and azimuth angles, because angular distances have equal scale over the image. The second formula is called **equi-solid angle projection**, and is used for estimating cloud obscuration and obstruction by buildings. The projected surface on the image plane scales linearly with the projected area on the sky.

Apart from these two projection formulas, two others are known for fisheye lenses:

$$r = f\sin(\theta) \tag{4}$$

$$r = 2f\tan(\theta/2) \tag{5}$$

Formula (4) is called **orthographic projection**, and this is a very special one. It is used to measure the illuminance on a plane surface perpendicular to the image plane, being the ratio of the unobstructed fraction of the sky to the total hemisphere. This is called the Sky View Factor, SVF, and is used in architecture. This projection has the additional property that the brightness of an object is equal everywhere on the image. This type of fisheye is rare and the Nikkor 10 mm $f/5.6$ OP is an example. It is better to avoid this type for meteor work because the image scale decreases strongly at large viewing angles, and is even zero at 180°.

Formula (5) is called the **stereographic projection**. It has the characteristic that angles between curves are preserved (though the area is not). Small objects therefore look very natural. So far I know there is no modern lens manufacturer offering this type of fisheye lens.

Figure 4 shows for all described projection formulas the image size as function of the viewing angle, assumed that they all have the same focal length. If you have a choice, the equidistant projection is preferable for meteor work because the compression at the horizon is least and, due to the simple projection formula, measurements on the film are straightforward. Figure 5 shows three pictures of the same spot, but with different fisheye types to illustrate their differences.

Despite the wide choice of projection formulas, in practice the lens never exactly matches the formula. This is illustrated in Table 1, where the real behaviour of an equidistant Nikkor 8 mm $f/2.8$ lens is given.

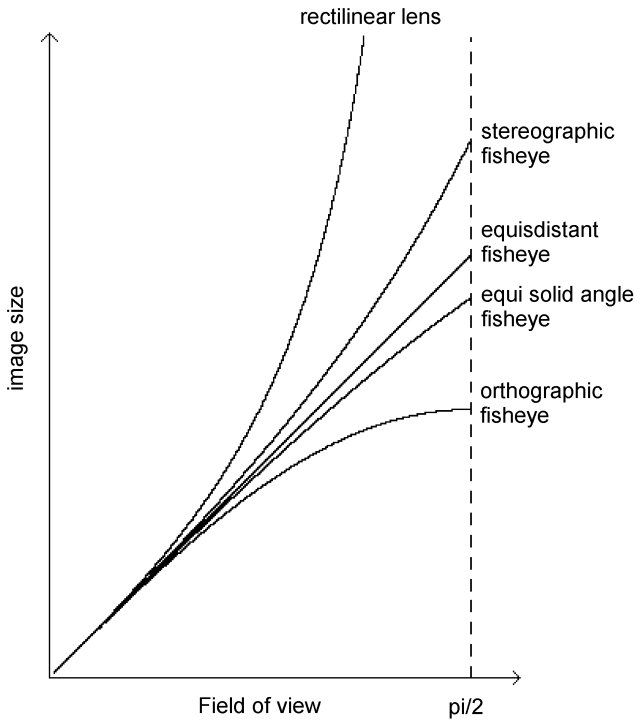

Figure 4 – Comparison of distortion of a rectilinear lens and different fisheye projections, assuming that they all have the same focal length.

Table 1 – Equidistant Nikkor 8 mm $f/2.8$ fisheye. r: distance from center of image plane; θ: viewing angle, $\Delta\theta$: difference from the previous value. For a real equidistant lens, $\Delta\theta$ would be invariant.

r	θ	$\Delta\theta$	r	θ	$\Delta\theta$
0.0	0.00	3.58	6.0	43.98	3.81
0.5	3.58	3.58	6.5	47.83	3.85
1.0	7.17	3.59	7.0	51.73	3.90
1.5	10.76	3.59	7.5	55.67	3.94
2.0	14.36	3.60	8.0	59.67	4.00
2.5	17.98	3.62	8.5	63.72	4.05
3.0	21.62	3.64	9.0	67.84	4.12
3.5	25.27	3.65	9.5	72.03	4.19
4.0	28.95	3.68	10.0	76.31	4.28
4.5	32.66	3.71	10.5	80.69	4.38
5.0	36.40	3.74	11.0	85.21	4.52
5.5	40.17	3.77	11.5	89.97	4.76

6 Efficiency for meteors

The efficiency of a lens with respect to meteors depends on two parameters: the diameter D and focal length f. For meteors the factor $D^2 f^{-1}$ is a measure of the sensitivity for meteors: with a larger aperture D^2, more light enters the lens; with a smaller f the meteor moves more slowly over the film, giving more light per film grain. In order to calculate the limiting magnitude for meteors, the formula generally used (Rendtel, 1993) is:

$$\mathrm{Lm} = 2.512\log_{10}(D^2 f^{-1} g) - 9.95 \tag{6}$$

where g is the sensitivity of the film in ISO.

To compute the efficiency of the lens we have to take into account the angular field A of the lens as well, which scales with f^2 for rectilinear lenses. For fisheye

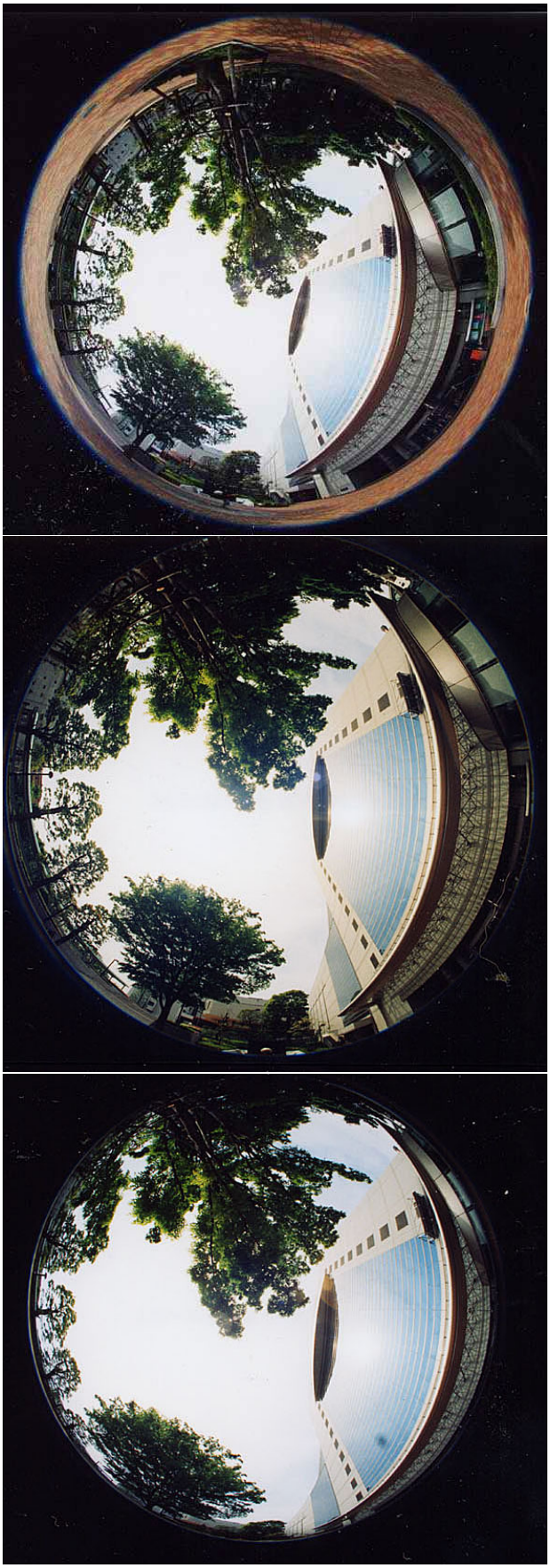

Figure 5 – Images of made with 3 different fisheye lenses: (a) Equidistant 6 mm with 220° FoV, tiles on the street are visible. (b) Equidistant 8 mm with 180° FoV, tiles are not visible anymore, the edge of the image equals horizon. (c) 10 mm orthographic lens, the image compresses strongly towards the horizon, the scale decreases to zero at the horizon.

Table 2 – Efficiency of lenses for meteors. 'FE' means fisheye lens. f: focal length in mm; f/D: focal ratio; D: lens diameter; Lm: limiting magnitude for meteors; A: field of view in square degrees; X: number of meteors in the time taken for a 50 mm $f/2.8$ to catch one.

	f	f/D	D	D^2/f	Lm	A	X
24 mm × 36 mm							
	28	2.8	10.0	3.6	−1.3	3038	2
	35	2.8	12.5	4.5	−1.0	2060	4
	50	1.4	35.7	25.5	+0.9	1069	7
FE	8	2.8	2.9	1.1	−2.6	20625	3
FE	16	2.8	5.7	2.0	−1.9	12062	3
58 mm × 58 mm							
	80	2.8	28.7	10.3	−0.1	1588	3
FE	16	2.8	5.7	2.0	−1.9	20625	5
FE	30	3.5	8.6	2.5	−1.7	13366	5
80 mm							
FE	30	3.5	8.6	2.5	−1.7	20625	7

lenses we have to take the projection formula into account to compute A. The following formula can be used to calculate the ratio of the efficiencies of a trivial lens and a 50 mm $f/2.8$ lens (Rendtel, 1993):

$$\begin{aligned} X &= \eta(\text{lens})/\eta(50\text{mm, f/2.8}) \\ &= A(D^2 f^{-1})^{1.21} f^{0.056} 10^{-4} \end{aligned} \quad (7)$$

Table 2 lists Lm and X for both wide angle lenses and common fisheye lenses. For reference, standard lenses are listed too. Compared to wide angle lenses, fisheye lenses do have a worse Lm but their enormous field compensates in terms of efficiency. It can be seen that for fisheye lenses the 30 mm type has the smallest negative (i.e. faintest) Lm. These lenses have another advantage: due to the larger focal ratio ($f/3.5$ instead of $f/2.8$ for the other listed ones), the sensitivity of sky background is less. Hence, exposures can last longer before the film saturates.

7 Plate reduction and accuracy

The process of extracting the coordinates (in right ascension and declination) of the meteor trail is called **plate reduction**. Despite the fact that it looks straightforward it is in practice rather complicated, especially for fisheye lenses due to their noticeable distortion. The essence of plate reduction is to compute a number of plate constants which describe all the characteristic parameters (such as magnification in x- and y-direction, image shift, rotation and distortion) for the transformation from image coordinates into hemispherical coordinates. A number of models exist, ranging from a linear plate model combined with the fisheye projection formula (Bettonvil, 2004), to second order plate models (Steyaert, 1990) and exponential ones (Ceplecha, 1987). In all cases the orientation of the camera (i.e. plate centre, which for all-sky instruments is always zenith) plays a role but is not precisely known. By iteration the best plate centre is found as an alternative to levelling the camera extremely precisely. Borovička (1992) published a method which is insensitive to the orientation.

Figure 6 – Nikon Coolpix 4500 with FC-E8 fisheye converter.

The accuracy with which one can calculate the coordinates of an arbitrary point is listed in Table 3 for several lenses. Fisheye lenses with a long focal length have the highest accuracies. For a 30 mm fisheye lens the achievable accuracy is typically 2–3′ and when doing precise measurements, even with high speed 400 ISO films, accuracies of 1′ are realistic. Measurements made on Canon 7.5 mm $f/5.6$ images provided 5′ with a 400 ISO film (Bettonvil, 2004). Basically the accuracy should scale linearly with the focal length, nevertheless the quality of the lens plays a role too. Plate reduction tests with a Nikkor 8 mm $f/2.8$, Nikkor 16 mm $f/2.8$ and Zodiak 30 mm $f/3.5$ under equal conditions showed equal performance for the 16 and 30 mm lenses, with the 8 mm being almost twice as bad. The Zodiak lens is an extremely cheap lens compared to both Nikkors (sometimes offered for around €250) but can compete with the Nikkor 16 mm.

In spite of everything, even expensive lenses do show aberrations, as was visible at the extreme edge of the Nikkor 16 mm. The Zeiss Distagon 30 mm $f/3.5$ is recognized as the highest quality lens available. Anti-reflection coatings are an important issue for fisheye lenses too: having a hemispherical view, it is impossible to avoid bright light sources such as the moon in the field of view, and these often cause multiple ghost images. Kumler (2000) tested several fisheye lenses for distortion and vignetting.

8 Fisheye lenses for digital photography

So far we have looked at fisheye lenses designed for conventional photography. In practice digital cameras cannot be equipped with these. Even when lens and camera have the same mount, the full fisheye effect is never reached because the size of the CCD or CMOS sensor is smaller (the biggest ones now being 15×23 mm) than the 24×36 mm of 35 mm film. The technology of digital photography develops extremely fast. For high accuracy work, however, film cameras are nowadays still preferable.

Recently Nikon presented their first digital fisheye lens for their D70, D100, D2 range: a 10.5 mm $f/2.8$ lens, which is the equivalent of the 16 mm $f/2.8$ in film photography. Nikon has circular fisheye converters on the market too, especially designed for one camera series (Coolpix), see Figure 6, with a reasonable quality and which have a full 180° field.

Table 3 – Astrometric accuracy (in arcminutes) for different combinations of films and lenses (Rendtel, 1993).

Film speed ISO	All sky mirror	Fisheye $f =$ 30 mm	Super wide angle $f =$ 20 mm	Wide angle $f =$ 35 mm
50	40	1	2	0.5
100	60	2	3	1
200	90	3	4	2
400	120	5	5	3

9 Conclusions

For all-sky imaging the fisheye lens is a good choice. There is a wide choice of fisheye lenses ranging from few hundred Euro (Zodiak) to over €5000 (Zeiss Distagon). For meteor work, lenses with a longer focal length are to be preferred as they give the most accurate results. Fisheye converters should be avoided because of their unsatisfactory quality.

References

Bettonvil F. (2004). "Nogmaals de trimultane vuurbol van 15 augustus 2002: sporadische oorsprong?". *De Meteoor*, **60**, 63–72. In Dutch.

Borovička J. (1992). "Astrometry with all-sky cameras". Technical Report 79, Publ. of the Astron. Inst. of the Czech. Academy of Sciences.

Ceplecha Z. (1987). "Geometric, dynamic, orbital and photometric data on meteoroids from photographic fireball networks". *Bull. Astron. Czech.*, **38**, 222–234.

Coastal Optical Systems Inc. (2005). `www.coastalopt.com`.

Gasden M. (1978). "Reflecting all-sky cameras". *J. Brit. Astron. Assoc*, **88:6**, 570–577.

Kumler J. (2000). "Fisheye lens designs and their relative performance". In Fischer R., Johnson R., Smith W., and Swantner W., editors, *Current Developments in Lens Design and Optical Systems Engineering*, volume 4093, pages 360–369.

Laikin M. (2001). *Lens Design.* Marcel Dekker Inc,. New York.

Miyamoto K. (1964). "Fisheye lens". *Journal of the Optical Sociey of America*, **54**, 1060.

Rendtel J. (1993). *Handbook for Photographic Meteor Observations, Monograph No. 3.* International Meteor Organization, Belgium.

Steyaert C. (1990). *Photographic Astrometry, Monograph No. 1.* International Meteor Organization, Belgium.

Vorst J. (1978). *Het Nikon reflex boek.* Elsevier, Amsterdam. In Dutch.

A review of video meteor detection and analysis software

Sirko Molau [1] *and Peter S. Gural* [2]

A software review is presented covering the topics of video meteor detection and post-detection analysis. This includes an overview of the algorithmic techniques and software packages currently available to the video meteor community.

Received 2005 February 23

1 Introduction

Meteor observations that are made using video collection systems have been gaining increasing attention and popularity within the meteor community. One reason is a growing awareness of the capabilities of this technique when using state-of-the-art CCD equipment. In particular, the light sensitivity of video systems has improved dramatically. Their application now extends from telescopic systems with arc-second accuracy and limiting magnitudes far beyond human visual acuity, to all-sky cameras with limiting magnitudes far beyond photographic limits. Thus an image intensified video system can be used for almost every aspect of meteor research in the optical domain.

Another reason for video's growing popularity is that highly sensitive (non-intensified) video systems have become available at reasonable prices. Our experience is that they are currently inferior to image-intensified systems by about a factor of three when the comparison is based on the number of meteor detections per hour. However, the low-light sensitive CCD cameras are very popular in the amateur-astronomical community because of their wide range of application (planetary imaging, occultation timing, lunar impact monitoring, etc.), their low price, ease of use, light weight, robustness, long lifetime and availability. So it comes as no surprise that non-intensified cameras outnumber the intensified systems by a ratio of two to one in the IMO Video Meteor Network.

Last but not least, it is of great help that software packages for automated meteor detection and analysis have been developed and are now readily available. Ten years ago, when meteor detection and analysis software was in its infancy, video observations were completed once the data was recorded on tape and a daunting analysis stage would begin. It was a tedious and time-consuming job to review the tapes manually, detect, and then measure the meteors by hand to prepare the data for further analyses. Today, a number of video systems are operated autonomously. In a typical set up, meteor imagery is fed in real-time directly to a personal computer, the meteor events are identified through specialized detection software, the meteor tracks are saved and analysed with post-detection software, and the results transmitted and maintained at central sites. Thus it has become a simple matter to feed the data from tens of thousands of video meteors into analysis software like Radiant to conduct detailed meteor shower investigations. It has never been easier for a newcomer to become a video observer and contribute valuable meteor observations.

[1] Abenstalstr. 13b, 84072 Seysdorf, Germany.
Email: sirko@molau.de
[2] 351 Samantha Dr., Sterling, VA 20164-5539, USA.
Email: peter.s.gural@saic.com

2 Meteor detection and analysis algorithms

There are a number of meteor detection and analysis software packages available to the video observer. Even though the software packages differ from one another in many aspects, they share a number of basic steps in common, which will be described here. Not all steps are implemented in each case — some packages stop after the meteor detection, whereas others only deal with the post-detection meteor analysis. Thus an end-to-end detection and analysis capability, as used by automated camera systems, requires a combination of these.

2.1 Image acquisition

The output of a frame-rate CCD video camera is typically a PAL or NTSC video signal that is either stored on videotape for later analysis, or streamed directly into the computer. In most cases, a frame grabber is used as the interface to digitize the video signal, resulting in a sequence of video frames stored in computer memory at rates of 25 or 30 frames per second (PAL or NTSC respectively). In a real-time system, the data stream (either live or played back from tape) is immediately processed by the meteor detection software. Alternatively, pre-recorded videotape can be transferred to a computer's hard disk in a standard video format (e.g. AVI, MPG) for later offline (non-real-time) processing.

Note that digital CCD cameras are becoming available on the market which will require a different and less expensive interface from camera to the computer. IEEE 1394 ('firewire') or USB 2.0 ports provide the connection between imager and computer memory or a hard disk. This technology is where the next generation of video meteor instrumentation is heading once the prices for digital cameras come down to make them more affordable to amateurs.

2.2 Image processing — clutter suppression

A number of image pre-processing steps are typically applied to the image stream to remove background clutter and improve meteor detection performance. Very often the optimal choice is highly dependent on the computer's processing capabilities and the application scenario. Typical steps are:

- **Spatial averaging:** 2x2 pixel averages may be used to lower the noise variance and decrease im-

age size by a factor of four to permit real-time processing on slower PCs.

- **Masking:** Regions of the image are masked out which are not relevant for meteor detection or that may produce false alarms. Examples are the area outside an intensifier's output field of view or a time stamp superimposed on the image.
- **Mean subtraction or frame differencing:** To remove non-moving objects such as stars, either a mean image is subtracted from each video frame or two adjacent frames in time are differenced. The mean image is typically derived from a number of previous video frames. For difference frames the absolute value is taken to ensure a meteor segment always appears as a higher signal level than the noise.
- **Variance normalization or flat fielding:** To achieve equal detection probability across the entire field of view, it is useful to normalize each pixel by its variance. The result is that noisy pixels are suppressed to a greater degree than those with smaller background fluctuations.

2.3 Image processing — meteor detection

The second stage of processing involves algorithms to decide whether a processed frame or sequence of frames contains a meteor or not. Typical steps are:

- **Clustering and thresholding:** After clutter suppression, a meteor should stand out as a bright spot or trailed line segment in the processed frame. Thresholding is used to decide whether a pixel or a set of adjacent pixels (region of interest, ROI) is to be considered as part of a meteor, or whether it is just noise. The threshold is adapted to the noise in the image in order to ensure optimum detection performance, i.e. to detect as many meteors as possible with only a few false alarms. The threshold can vary both spatially across the image and temporally in time to account for changing scene conditions.
- **Spatial correlation:** This approach enhances the signal energy by taking advantage of the linear trailed shape of meteors in a single video frame. Small line segment templates for a variety of orientations can be applied to the imagery with a threshold set that flags regions with linear features. Alternatively a Hough transform of pixels that exceeded the threshold can be calculated which maps linear features in an image into peaks in Hough space, which in turn can be thresholded to flag candidate meteor tracks.
- **Temporal correlation:** Unlike noise, meteors typically appear as line segments that propagate across several video frames. The threshold for meteor detection can be lowered significantly, if meteors are required to be detected in a number of sequential frames. A further constraint can be that the individual meteor detections follow a straight line with approximately constant spacing and a resulting uniform angular velocity that falls within the valid range for meteors. The temporal correlation can be done via a tracker that pieces together detections from a sequence of individual frames that meet an association criterion for linear propagation. Alternatively, a matched filter can be used that integrates the meteor track in both space and time given a suspected orientation, speed, and position (e.g. from a Hough transform peak).

2.4 Data storage

The output of a meteor detector is typically the time of a meteor and a short frame sequence of the object. Since the relative position of the meteor in the video frame is known, it is often sufficient to save only the region around the meteor. By not writing full video frames, most of the software packages save disk writing time in real-time operations as well as minimizing the hard disk storage used.

2.5 Astrometry and photometry

Astrometry and photometry are the first steps of post-detection meteor analysis. By means of standardized procedures, the relative position of the meteor is transformed into equatorial coordinates, and the meteor's integrated light intensity (distributed pixel sum less background) is transformed into magnitudes. For real-time processing it is often sufficient to measure the reference stars for astrometry and photometry once before the start of observation. In the case of offline analyses, the reference stars may be measured individually for each separate meteor to provide a higher level of measurement precision.

2.6 Single station analysis

From the individual measurements in each frame, a mean meteor path and a light curve can be computed. The apparent angular velocity is derived from the path length of the meteor, the frame rate, and the calibrated image scale. The same algorithms that are used for the data reduction of visual meteor observations can also be used to associate video meteors to known showers. Some real-time detection packages actually do radiant association of the meteors on the fly by knowing the time of the initial astrometry and using the computer's onboard clock to update the reference field and sky orientation within the field of view. Final results may be stored in a simple text file, in a standard format like IMO's PosDat format, or in some proprietary database format. In the case of automated meteor detection it often makes sense to manually inspect the detections later on, in order to reject false alarms by airplanes, satellites, birds, insects and other image artefacts.

2.7 Multi station analysis

If observations from more than one station are available, multiple detections of the same meteor by different stations need to be identified (initially through temporal

coincidence). This is typically done offline. Afterwards, standard algorithms for orbit calculation are applied to obtain the orbital parameters of the meteoroid. If the single station analysis was performed automatically, it may be necessary to revise the individual meteor positions in order to achieve maximum accuracy.

2.8 Additional tools

Meteor analysis software may come as software packages in connection with add-on tools. These can be used to prepare for an observation (e.g. digitize and measure a reference image or define an optimal station configuration in two-station observations), to perform parts of the meteor analysis (astrometry, photometry), to review the results (e.g. remove false detections), or estimate orbital parameters from a multi-station meteor track.

3 Meteor detection and analysis software

In the following, four meteor detection and analysis software packages will be introduced and compared. We concentrate on programs that implement most steps of video meteor analysis, that are easily available and that are widely in use. We are aware that there is other software for the meteor enthusiast to perform both pre- and post-detection analysis. As an example, we would like to mention a number of programs that can perform orbital element estimation by applying all the standard meteor correction factors given multiple camera measurements.

3.1 MetRec

MetRec is a full-featured real-time meteor detection and analysis software package. The first version of MetRec became available in 1998, but the roots date back to 1993, when a predecessor code for automatic meteor detection and analysis was implemented. Since it's first release, MetRec has been further enhanced and completed. The focus of MetRec is to support autonomous operation of a video meteor camera over a long period of time. Only a minimum amount of manual interaction is required for preparation and post-processing of observations, which is supported by additional tools. MetRec has many configurable parameters that allows for good adaptation to different video systems and tasks. The detection probability is well above 80%. MetRec has highly optimised routines and runs on a 500 MHz Pentium PC with full performance. The software is widely used in the meteor community. Camera networks like the IMO Video Meteor Network, the video network of the Denver Museum of Science and History in the USA, and the Polish fireball network are based on the MetRec software package. In addition, MetRec is used by a number of individual observers and astronomical institutes.

Currently, MetRec does not include multi-station observation, but additional tools were developed at ESA that take the output files of MetRec and compute orbital parameters from double-station observations. MetRec requires either a 'Meteor' or 'Meteor II' frame grabber built by Matrox Corporation, and is currently configured to run under MSDOS, Windows95, and Windows98 only.

3.2 MeteorScan

MeteorScan is another full-featured meteor detection and analysis software package. The first version was published in 1996 with major upgrades taking place during the Leonid ground and airborne campaigns of 1998 through 2002. The real-time version executes on the Macintosh line of computers working with streaming analog video through a Scion Corporation LG-3 frame grabber. The offline version executes on a PC working from AVI video files that were streamed to hard disk from pre-recorded digital video via an IEEE 1394 (firewire) interface. One special feature of MeteorScan is its ability to adapt to both ground and airborne observing conditions. Using frame differencing and pixel specific noise tracking (i.e. special types of stationary object removal and flat-fielding) allows the software to deal with the drifting star fields typically experienced on airborne sensor platforms and in very narrow field-of-view ground-based meteor imaging. The masking, astrometry calibration, meteor scanning and detection, meteor track user confirmation, replay, and reporting functions are all seamlessly integrated into a single package.

The real-time (Mac) version runs with a minimum of interaction to support nightly autonomous operation. The real-time version was also designed to be automatically adaptable to adjust for faster processor speeds so that probability of detection (Pd) improves with Moore's Law. For a 300 MHz Macintosh, Pd's of better than 80% were easily achieved in the late 1990's. The offline (PC) version, which runs under any Windows OS, is not time constrained as it reads imagery directly from hard disk. Thus the real-time processing restrictions have been relaxed with a resulting Pd of 99%. Current estimates indicate that a 3 GHz PC would achieve this detection rate operating in a real-time processing mode. Planned work involves interfacing the PC version to live digital video providing real-time, automated, and high probability of meteor detection using state-of the-art video technology.

The MeteorScan software is in use by professional meteor researchers in the USA at NASA/Marshall, the SETI Institute, and Aerospace Corporation as well as in Canada at the University of Western Ontario and Mount Allison University. Spin-offs of the real-time processing software have been applied to massive compact halo object detection (MachoScan), lunar meteoroid impact flash detection (LunarScan), and a mirror-based meteor-tracking spectrometer and orbit estimation system (MeteorCue), the latter of which is based on a very fast cluster detection algorithm rather than the Hough transform/matched filter employed in MeteorScan.

Software	**MetRec**	**MeteorScan**	**Astro Record**	**UFOCapture tool set**
Author	S. Molau / Germany	P. Gural / USA	M. deLignie / Netherlands	SonotaCo [1] / Japan
Download or contact address	`http://www.metrec.org`	`peter.s.gural@saic.com`	`http://www.imo.net` [2]	`http://www65.tok2.com/home2/SonotaCo/`
Minimum hardware requirements	Pentium PC, 200 MHz, 16 MB RAM	Online: Mac, 300 MHz, 64MB RAM Offline: PC, 300 MHz, 64MB, IEEE 1394 video board, 25 GB disk space	486 PC, 33 MHz, 8 MB RAM	Pentium PC, 2 GHz, 512 MB RAM
Recommended hardware	Pentium PC, 600 MHz, 32 MB RAM	Mac: the fastest speed processor for highest real-time Pd	Pentium PC, 600 MHz, 32 MB RAM	Pentium PC, > 2.4 GHz, > 512 MB RAM
Framegrabber / interface	Matrox Meteor / Meteor II	Mac: Scion LG-3 framegrabber PC: IEEE1394	—	Any DirectX-compatible video capture device or interface
Operating System	DOS, Windows 95/98	Mac: Mac OS 7.5.3 or later PC: Windows 95 or later	Windows 3.x,95/98/NT/ME/ 2000/XP	Windows XP/2000/ME (English and Japanese)
Image acquisition and input	Online: PAL & NTSC video camera or tape	Online: PAL & NTSC video camera or tape Offline: AVI	Offline: BMP, PCD, AVI	Online: PAL & NTSC with PCI framegrabber, non-standard signal (e.g. VGA from webcams) [3] Offline: AVI, WMV
Internal resolution	384x288 x 25 fps (PAL) 320x240 x 33 fps (NTSC)	768x576 x 25 fps (PAL) 640x480 x 30 fps (NTSC)	—	UFOCaptureFree: up to 320x240 x 30 fps UFOCapturePro: up to 720x480 x 30 fps
Meteor detection	Real-time (Pd > 80%): – pixel averaging – masking – mean subtraction – variance normalization – small region template matching – pixel clustering – thresholding – tracking of multiframe ROI	Real-time (Pd> 80%), Offline (Pd=99%) (for <20% false alarm rate): – masking – frame differencing – variance dependent thresholding – multi-frame Hough integration which cues a space-time matched filter	—	Detection real-time, classification offline – masking bright stationary objects – thresholding within the detection area
Data storage	Meteor images, sequence (meteor only), individual meteor frames	Meteor images, sequence (meteor only), individual meteor frames	—	Meteor images, frame sequence
Data format	Images: BMP Sequences: internal format	Images: TIFF Sequences: internal format	Same as original	Images: BMP Sequences: AVI

Software	**MetRec**	**MeteorScan**	**Astro Record**	**UFOCapture tool set**
Photometry / astrometry	Automatic, real-time, 1st ... 3rd order polynomial fit	Automatic, real-time, 2nd order polynomial fit	Manual, offline, 1st ... 3rd order polynomial fit	Automatic, offline, discrete coordinate transformation (no fit) with 3rd order radial symmetric distortion function
Single station analysis	Position, brightness, velocity, radiant association	Position, brightness, velocity, radiant association (this last for ground based systems only)	Position, brightest point, average velocity	Position, brightness,velocity, radiant association
Data format	ASCII, PosDat (dBase)	ASCII	ASCII	ASCII (CSV)
Multi-station analysis	— [4]	—	— [5]	Automatic with the UFOorbit tool (currently elliptical orbits only)
Special features	– Supports fully autonomous video meteor observation – Can be adapted manually and automatically to different camera systems and conditions – Low hardware requirements – Recognition of superimposed time-signal synchronized clock – Includes Tycho star catalog down to $m = 8$ and lunar / solar ephemeris – Real-time display of star map with meteor trails and radiant association statistics	– Supports fully autonomous video meteor detection – Auto-adapts to variable background and camera characteristics – Includes UBVRI stellar catalog to magnitude +9.0 – Automatically improves Pd as processor speed increases – Easy resumption of operations from previous session – Real-time display of radiant association statistics	– Same interface for measuring photographic and video observations – Uses Sky Catalogue 2000.0, Vol. 1 – Possibility to repeat the measurements for enhanced accuracy	– Multipurpose software which can detect more than meteors – Fast software development – Can use any DirectX video capture device (PCI framegrabber, IEEE 1394, USB) – Ground map (Japan only) for multi station analysis – Includes Yale Bright Star catalogue V. 5
Additional tools	– Digitization and measurement of reference images for photometry/astrometry – Post-processing of observations – Creation of time-lapse movies – Real-time measurement of stellar lightcurves (for occultations)	– Point and click astrometry for FOV/magnitude calibration – Adjustable masking (e.g. time stamp) and thresholds – User confirmation of meteor detections – Playback of detected meteor video segments	—	– Meteor analysis is carried out by a set of tools (UFOCapture, UFOAnalyser, UFOOrbit) – Alarm the user when objects are detected
Language	GUI: English Docs: English / Japanese	GUI & Docs: English	GUI & Docs: English	GUI: English Docs: Japanese
Costs	Amateurs: none Professionals: €250	None, software upgrades are price negotiable	None	UFOCapture Free: none UFOCapturePro: ca. €30

Footnotes: see Table 1 on page 20.

3.3 Astro Record

The Astro Record program is aimed at making position measurements of celestial objects, especially meteors, and performing the associated astrometric calculations. For this purpose, screen coordinates of the object and of a number of reference stars can be measured, equatorial coordinates of the reference stars can be looked up, and the results of the astrometric calculations can be analysed regarding wrong star identifications and plate defects. The results are stored in an output file that can be used by the Turner astrometric computer program in use by the Dutch Meteor Society for multi-station analysis. In addition, the equatorial coordinates of each meteor's begin and end points are stored in a log file that can easily be converted to IMO's PosDat format.

The program can handle photographic images in the BMP and PCD (Kodak Photo CD) format as well as AVI video sequences. The data entry of equatorial coordinates is eased by the possibility of specifying a constellation name and Flamsteed number. From the fourth star onwards, the program predicts the most probable star from a list of possible stars, based upon the previous measurements. The user can choose between a first, second or third order polynomial fit to convert local x,y pixel coordinates to equatorial coordinates (Turner's method). A third order fit can compensate for the most common image distortions due to camera and projection lenses, Photo CD production, optical scanning, image intensifiers, etc.

3.4 UFOCapture tool set

UFOCapture is a software package designed to detect moving objects. It comes in two versions, the limited-resolution freeware version 'UFOCaptureFree' and the full-resolution shareware version 'UFOCapturePro'. UFOCapture can be used to record meteors, sprites, Iridium flares, satellites and other objects. The detection algorithm is not tuned specifically towards meteor detection and therefore uses algorithms slightly different than those described above. Instead of masking regions that are not suitable for meteor detection, up to four rectangular regions can be defined for object detection. Mean subtraction or differentiation, variance normalization and spatial / temporal correlation are not applied, but instead bright stationary objects are masked out in real-time from the image. Remaining objects that are then brighter than a given threshold are classified as moving objects and a short AVI sequence is saved.

A number of additional tools are under development that will make the UFOCapture tool set a more full-featured meteor analysis software package. They are available in preliminary releases, which are upgraded in short succession. UFOAnalyser classifies the detected objects offline (e.g. meteor, airplane, insect), which takes about one to ten seconds per sequence. Each object class is defined by a number of configurable parameters like brightness, size and duration. After classification, the result can be revised manually. For astrometry purposes, a star map is superimposed on the image. The user adapts the parameters of the map (size, rotation, center of the field of view, distortion) manually until a best fit to the image is obtained. The resulting parameters are used for single station analysis (astrometry, photometry) with final results written to a text file. UFOOrbit is another tool, which reads the text file from UFOAnalyser, looks for meteor pairs from different camera systems, and does a multi station analysis (elliptical orbits only). The result can be displayed in terms of radiant, trail, ground and orbit maps. Finally, UFOWatchdog can be used to monitor the operation of UFOCapture and notify the observer if moving objects are detected.

Overall, the UFOCapture tool set is based on DirectX and therefore supports a wide variety of input sources and capture devices, but requires state-of-the-art PC hardware. The tool set is relatively young and still under development, but is used already by about 20 active Japanese video observers.

The software is summarised in the Table on pages 18 and 19, the footnotes to which follow.

[1] Nickname of the anonymous programmer.
[2] The 16-bit version is available from www.imo.net. A 32-bit version is available by contacting the author.
[3] No IEEE1394 support for PAL.
[4] Additional software for double station analysis, which uses the MetRec output files, is available at ESA SSD.
[5] Output files interface with the multi-station analysis software of the Dutch Meteor Society, which is based on the software developed at the Ondrejov Observatory in the Czech Republic.

4 Summary

More than a decade after the first steps towards computer-based video meteor detection and analysis, a number of specialized software packages are available in different languages (mostly English and Japanese). They support both automated real-time observation as well as high-accuracy manual off-line analysis. Even though each of these programs has certain features and characteristics, they all share some basic functions.

The number of both professional and amateur video systems is increasing, and camera networks have collected already hundreds of thousands of meteor records. It has never been easier and cheaper to become a video meteor observer. We would like to encourage and invite you to build and operate your own video system and contribute valuable single or multi-station data for ongoing meteor science projects.

Acknowledgements

The authors would like to thank M. deLignie for the input on the Astro Record software, and Miyuki Shishido for providing information on the UFOCapture tool set.

Results of ten years of photographic meteor spectroscopy (1994–2003)

Miloš Weber [1]

Observing data and a brief description of five meteor spectra, obtained during the period 1994–2003, are presented.

Received 2004 February

1 Introduction

The writer, a former visual observer, has conducted a program of systematic meteor spectrum photography at a private observing site at Chouzavá (Latitude 49°50′ N, Longitude 14°13′ E). An aim was that the limiting meteor magnitude of recorded spectra should match that of the all-sky cameras used for direct meteor photography by the Czech network (about $m = -4$). This program has supplied results to the Czech network, as all the spectra obtained were given to Dr. J. Borovička, Ondřejov Observatory, for measurement and analysis (Borovička, 1993; Borovička, 1994).

2 Instruments and observing data

Two cameras operated in a fixed regime were used: Camera X with an $f/3.5$, $f = 150$ mm lens and a 30° objective prism and Camera T with an $f/4.5$, $f = 165$ mm lens and a 45° objective prism. Both cameras were provided with the same rotating shutter, 10 breaks/s. Sheet films of 9×12 cm with sensitivities of 100, 200 and 400 ASA were used (Guth, 1940).

2.1 Review of meteor spectrum exposures

Exposed in 1994–2003 during 202 nights:

Camera	Time (hours)	Films used	Spectra obtained
X	716.6	220	4
T	507.1	155	2
Totals	1223.7	375	6 from 5 meteors

Exposure needed for one spectrum:

Camera	Time (hours)
X	179.2
T	253.6
Average	204.0

For comparison, the 1932 – 1933 meteor spectrum campaign organised by P. M. Millman used three cameras similar to cameras X and T of this paper. During one year (and ignoring the great shower), they exposed a total of $1350\overset{\text{h}}{.}9$ on 788 photographic plates and obtained five spectra. The main differences between these two works are: the observing site Chouzavá is 420 m a.s.l. (above sea level), whereas Flagstaff is 2210 m a.s.l.. The sensitivity of the photographic material in 1933 was about 50 ASA (estimate by the present author); in the years 1994 to 2003 it was 100, 200 and 400 ASA.

A comparison of the average exposure time needed to obtain one meteor spectrum shows: $179\overset{\text{h}}{.}2$ for Camera X, $251\overset{\text{h}}{.}6$ for Camera T at Chouzavá, and an average of $279\overset{\text{h}}{.}2$ for the three cameras at Flagstaff (Millman, 1935).

3 Review of the spectra obtained

1. **'Kouřim' bolide** (Spurný, 1995; Spurný, 1997)
   Date: 1995 April 22, $22^{\text{h}}28^{\text{m}}40^{\text{s}}$ UT.
   Absolute magnitude: beginning −3.6; maximum −15; end −3.
   V_∞*:* 27.5 km/s.
   Spectrum: 29 lines; inclination to the edge of the prism 8°.
   Chemical composition: chondrite.
   Film: 100 ASA.

2. **'α Capricornid'** (Borovička & Weber, 1996)
   Date: 1995 August 02, $21^{\text{h}}48^{\text{m}}01^{\text{s}}$ UT.
   Apparent magnitude: beginning −2; maximum −5.
   V_∞*:* 22.8 km/s.
   Spectrum: 29 lines; inclination to the edge of the prism 71°.
   Chemical composition: of both chondrites and cometary material.
   Film: 100 ASA.

3. **'Perseid'**
   Date: 1997 August 09, $22^{\text{h}}58^{\text{m}}$ UT.
   Analysis: not yet analysed and published.
   Film: 100 ASA.

4. **'Vimperk' bolide** (Spurný & Borovička, 2001)
   Date: 2000 August 31, $22^{\text{h}}51^{\text{m}}56^{\text{s}}$ UT.
   Absolute magnitude: beginning −3.5; maximum −13.8; end −4.
   V_∞*:* 14.7 km/s.
   Spectrum: 7 lines (only the fireball beginning captured); inclination to the edge of the prism 73°.
   Chemical composition: chondrite.
   Film: 200 ASA.

5. **EN 260803 bolide**
   Date: 2003 August 26, $21^{\text{h}}37^{\text{m}}20^{\text{s}}$ UT.
   Apparent magnitude: beginning −3.3; maximum −5.4.
   V_∞*:* = 27.1 km/s.
   spectrum: 12 lines; inclination to the edge of the prism 60°.
   Analysis: not yet analysed, preliminary identification of calcium line.
   Chemical composition: probably chondrite.
   Film: 400 ASA.

[1]Verdunská 19, 16000 Praha 6 – Bubeneč, Czech Republic.

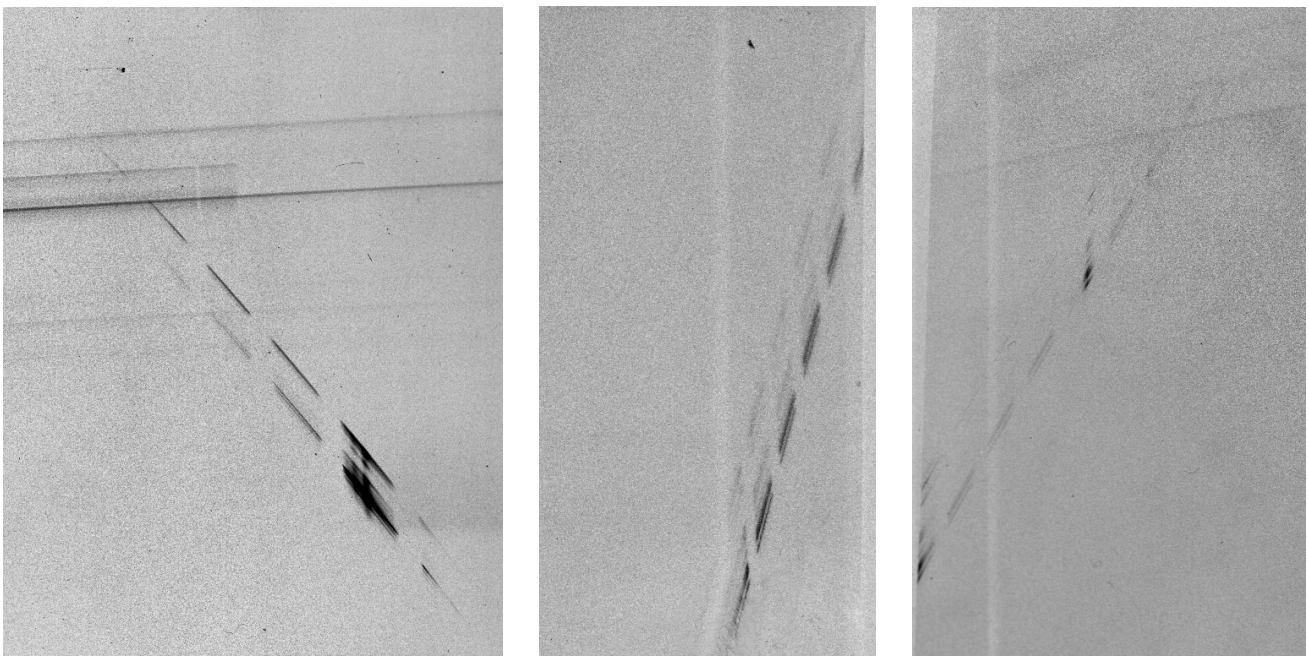

Figure 1 – Spectra photographed from Chouzavá, Czech Republic. All have 10 shutter breaks per second. **Left, spectrum 3:** a Perseid photographed on 1997 August 09, $22^{\rm h}58^{\rm m}$ UT with an $f/3.5$, $f = 150$ mm lens and a 30° prism. **Centre, spectrum 5:** the final part of a trail of a sporadic photographed on 2003 August 26, $21^{\rm h}37^{\rm m}20^{\rm s}$ UT with an $f/3.5$, $f = 150$ mm lens and a 30° prism. **Right, spectrum 5:** the middle part of a trail of the same sporadic photographed on 2003 August 26, $21^{\rm h}37^{\rm m}20^{\rm s}$ UT with an $f/4.5$, $f = 165$ mm lens and a 45° prism.

Spectra 1 and 3 complete the evidence from the spectral cameras at the Ondřejov observatory, whereas spectra 2 and 4 were even not recorded at Ondřejov, and spectrum 5 is better than the Ondřejov one. Spectrum 1 gives the short wavelength part to the two corresponding Ondřejov spectra. All spectra completed the entire set of parameters of these meteoroids, i.e. the atmospheric trajectory and heliocentric orbital data. Figure 1 shows spectra 3 and 5 which have not previously been published.

4 Conclusion

This paper has presented the results of 10 years of systematic meteor spectrum photography. During the years 1994–2003, six meteor spectra were recorded after $1223\overset{\rm h}{.}7$ of exposure in total. The average time needed for one spectrum was $204\overset{\rm h}{.}0$. Four of these six spectra were from slow meteoroids with V_∞ from 14.9 to 27.5 km/s. All six spectra showed the chemical composition of chondrite types. (This includes provisional analysis for spectra 3 and 5.) The same chemical composition was found in meteoroid 4 'Vimperk', which had the rare Aten type of orbit where some of the older recorded spectra showed an iron composition. All these six spectra are from the five instances where all the usual meteoroid parameters could be determined.

Acknowledgements

The author is indebted to Dr. J. Borovička and Dr. P. Spurný for their permanent helpful cooperation.

References

Borovička J. (1993). "A fireball spectrum analysis". *Astron. Astrophys.*, **279**, 627–645.

Borovička J. (1994). "Two components in meteor spectra". *Planet. Space Sci.*, **42**, 145–150.

Borovička J. and Weber M. (1996). "An α-Capricornid spectrum.". *WGN*, **24:1/2**, 30–32.

Guth V. (1940). *O fotografování meteorů*. Vyd. Meteor. sekce ČAS.

Millman P. M. (1935). "An analysis of meteor spectra. Second paper". *Annals of Harvard College Observatory*, **82:7**.

Spurný P. (1995). "O jednom velkém jarním bolidu". *Říše hvězd*, **76:9–10**, 176–178.

Spurný P. (1997). "Exceptional fireballs photographed in Central Europe during the period 1993 – 1996". *Planet. Sp. Sci.*, **45**, 541–555.

Spurný P. and Borovička J. (2001). "EN 310800 Vimperk fireball: Probable meteorite fall of an Aten type meteoroid.". In *Proc. Meteoroids 2001 Conf., 6–10 August 2001*, ESA SP-495, pages 519–524. Swedish Inst. of Space Physics, Kiruna, Sweden.

CCTV lenses for video meteor astronomy

Mariusz Wiśniewski [1], *Arkadiusz Olech* [2], *Mirosław Krasnowski* [3], *Kamil Złoczewski* [4], *Krzysztof Mularczyk* [5], *Piotr Kędzierski* [6], *and Wojciech Jonderko* [7]

We present the results of CCTV lens tests made last year at the Ostrowik Observatory by observers of the Comets and Meteors Workshop. A total of 13 lenses with different parameters were tested. The limiting magnitudes, size of field of view, distortion and off-axis aberrations were measured. The Computar $f/1.2$, $f = 4$ mm appeared to be the best lens tested. We also note the good marks of both Ernitecs which were finally chosen as the lenses which will be used in our projects. Surprisingly, the very fast lenses which are popular in video meteor astronomy seem to be much worse that their $f/1.2$ rivals.

1 Introduction

One of the key indispensable elements for video observations of meteors is a good lens. The quality of the resulting image of the sky depends not only on the detector characteristics but also on the lens quality. A poor lens can produce images with large off-axis optical aberrations, distortion and vignetting, causing problems with determining the properties of meteors observed at the edge of the field.

Lenses for CCTV (closed-circuit television) are cheap but quite complicated devices. Typically, their optics contain many lense elements made with different kinds of glass, with different shapes in different structures and arrangements. It is not easy to build a good quality instrument at that small size. Thus the lenses of different manufacturers with the same parameters could produce completely different results.

During the last two years, the Polish *Comets and Meteors Workshop (CMW)* started two projects which use video techniques extensively. These are the *Polish Automated Video Observations (PAVO)* project (Wiśniewski et al. 2003) and the *Polish Fireball Network* (Olech et al., in preparation). These projects are financially supported by Siemens Building Technologies and Factor Security. Of course the funds are limited and thus we are interested in buying only equipment with the best quality to price ratio. Thanks to Factor Security we had access to many CCTV lenses offered by this company and thus we decided to test their usefulness in meteor astronomy.

2 Parameters and properties

Optical parameters of CCTV lenses are described in the same way as for photographic lenses: f/x, where x is some number, tells us how fast a lens is[1] and $f = x$ is its focal length (for example $f/1.2$, $f = 8$ mm). The ratio of these gives us the diameter of a lens which is the most important factor in determining the amount of light gathered by our equipment.

There is relection and refraction of light at each air-to-glass surface. Of course we want to avoid reflection. The reflected light does not hit our detector, causes a decrease of the lens' optical efficiency and produces ghost images. In a typical air-to-glass surface about 95% of light goes through it but 5% is reflected. This looks as a small number, but typical lens contains more than 10 such surfaces. This gives us a transmission of $0.95^{10} \sim 0.60$ and as much as 40% of the light lost!

To solve this problem, manufacturers of optical instruments cover the lenses with thin layers of materials such as MgF_2, SiO_2 or TiO_2. The most sophisticated multilayer coatings made by top manufacturers can decrease the light loss at one air-to-glass surface even down to 0.2%.

3 Fighting the aberrations

Light going through lenses can suffer from the influence of many aberrations. We list them here briefly. For further details of these, see textbooks on optics such as (Hecht, 1998; Ray, 1977; Welford, 1991).

Chromatic aberration is the result of dispersion in the glass and occurs when shorter wavelength light is refracted more than longer wavelength. In other words a lens that suffers from chromatic aberration will have a different focal length for each color. In color CCTV cameras this produces violet rings around bright stars.

In most common cases, the surface of a single lens is a section of a sphere since this is the easiest shape to make. But with a spherical surface, incoming rays from different distances from the optical axis focus at slightly different points along the axis. So if the center of the image stays in focus and is bright, the edges of the field appear blurry and dimmer. This effect is called spherical aberration.

Coma (Latin, related to the origin of the word 'comet') is off-axis spherical aberration caused by rays entering the lens at an angle. Due to this phenomenon,

[1]Nicolaus Copernicus Astronomical Center, Bartycka 18, 00-716 Warsaw, Poland. Email: mwisniew@camk.edu.pl
[2]Nicolaus Copernicus Astronomical Center, Bartycka 18, 00-716 Warsaw, Poland. Email: olech@camk.edu.pl
[3]ul. Zjazd 6, Poznań, Poland. Email: mirek@post.pl
[4]Warsaw University Astronomical Observatory, Al. Ujazdowskie 4, 00-478 Warsaw, Poland.
Email: kzlocz@astrouw.edu.pl
[5]Warsaw University Astronomical Observatory, Al. Ujazdowskie 4, 00-478 Warsaw, Poland.
Email: kmularcz@astrouw.edu.pl
[6]Warsaw University Astronomical Observatory, Al. Ujazdowskie 4, 00-478 Warsaw, Poland.
[7]ul. Pod Walem 23, 44-203 Rybnik, Poland.
Email: wjonderko@go2.pl

[1]This strange but traditional notation describes the focal ratio f/d, where f is the focal length and d the lens diameter. For example '$f/1.2$, $f = 8$ mm' says that the diameter is $f/1.2$, i.e. 8/1.2 or 6.7 mm. *–Editor.*

Figure 1 – The 13 lenses tested.

point-like images of stars become blurry comet-like structures at the edge of the field of view.

Astigmatism is another off-axis aberration. The incoming rays passing through the lens at oblique angles with respect to the optical axis focus differently from paraxial rays. (See the *Glossary* below.) Depending on the incidence angle of the off-axis rays entering the lens, the refracted plane is oriented either tangentially or sagittally. So the resulting image depends upon the location in the focal plane and thus produces blurry images, more or less elongated, of which the intensity and contrast decrease as the distance from the center increases.

Distortion is an effect of the focal length of the lens varying with the distance from the optical axis. As a result some parts of the image are more magnified than others. Distortion occurs in two main forms: barrel and pincushion, also called negative and positive distortion respectively.

Glossary

Optical axis: the axis through the centre of all the lens elements, at right-angles to them.
Paraxial: a light ray not parallel to the optical axis, but at only a small angle to it.
Chief ray: a ray passing through the centre of a lens element, but at an angle to the optical axis.
Tangential: consider a plane which contains both the optical axis and the chief ray: this is the tangential plane. A ray within this plane, but not passing though the centre of the lens element, is a tangential ray.
Meridional (plane or ray): synonym for tangential (plane or ray).
Sagittal: consider a plane which contains the chief ray but is at right-angles to the tangential plane: this is the sagittal plane. A ray within this plane, but not passing though the centre of the lens element, is a sagittal ray.

Figure 2 – The experimental setup for the tests.

Table 1 – Basic parameters of the tested lenses. (a): auto iris (adjusts automatically to light level); (z): zoom. F: focal ratio, i.e. f/d. FWHM: stellar image width. Columns dist_1 and dist_2 are measured in percentages of the distance from the image center to the corner. For an explanation of other quantities, see the Section 4.

Name	f (mm)	F	FOV (°)	FWHM (pix)	LM_s (mag)	LM_l (mag)	OE %	$\mathrm{dist}_{\max}$ (pix)	dist_1 (%)	dist_2 (%)
ERNITEC (a)	2.8	1.4	120.8	1.82	0.70	6.26	49	-2.608	85	100
COMPUTAR	8.0	1.2	43.2	1.89	3.98	8.51	54	-2.654	78	100
SIEMENS	12.0	1.2	27.9	1.86	4.30	8.88	33	0.697	100	100
COMPUTAR	4.0	1.2	91.2	1.69	2.95	7.76	94	17.976	57	62
ERNITEC	8.0	1.2	42.1	1.52	3.65	8.55	47	-4.106	62	73
SIEMENS	4.0	1.2	85.6	1.84	2.30	6.88	47	12.536	66	76
PENTAX	8.0	1.2	42.1	2.18	3.41	8.57	43	1.998	92	100
SIEMENS	6.0	1.2	55.9	1.93	3.86	7.90	72	-7.934	62	69
TAMRON (z)	2.8	1.4	103.4	1.86	1.34	6.14	59	-18.150	53	59
EVETAR	12.0	1.4	29.7	2.25	3.65	8.50	28	-0.940	100	100
TAMRON (z)	3.0	1.0	115.2	2.00	1.84	6.43	38	-4.927	62	71
SIEMENS (a)	4.0	1.2	85.6	2.18	2.91	6.57	61	12.254	57	67
COMPUTAR (a)	3.8	0.8	90.9	2.72	2.06	5.74	14	4.946	64	74

The CCTV detector is always a flat plane but the resulting image plane given by the lens is not. This phenomenon is called field curvature and produces problems with obtaining sharp images across the whole field of view.

4 Tests

Our tests were made on 2004 February 21 at the Ostrowik station of Warsaw University Astronomical Observatory. In total, we tested the 13 lenses shown in Figure 1; their basic parameters are given in Table 1.

As a detector we used a monochrome Mintron MTV-13V3 camera with a frame integration function available. The images from the camera were recorded with a high quality Panasonic AG-TL300 video recorder. First, we checked the appearance of the sky for single frame normal mode. Second, we used the integration mode of the Mintron camera. We recorded images made by accumulating 128 frames. For normal and integrated modes the exposure times were of 0.02 and 2.56 sec, respectively. Integrated mode gave us a chance to see more faint stars and to find even slight differences between the limiting magnitudes of particular lenses. All the optical defects described above are more visible in integrated images. Our testing equipment is shown in Figure 2.

We used a Matrox Meteor II card to convert analog images into digital form. We used the grab program, which is a part of MetRec package (Molau 1994, 1995, Molau & Nitschke 1996, Molau et. al 1997). Examples of integrated images are shown in Figures 3 and 4. We grabbed images at the resolution of 384 × 288 pixels used by MetRec software. (This software halves the horizontal and vertical resolution with 2×2 binning.)

4.1 Image deformation

We looked for distortion effects on long exposure images. We used the Refstars program (Molau, 1992) to identify stars. Observed stars' positions were compared with the theoretical positions for ideal optics. The graphs showing the differences (in pixels) between the observed and correct positions of the stars as a function of the distance of the star from the center of the FOV (field of view, also in pixels) are shown in Figure 5 (page 29). The field sizes (in percentages of the distance from the image center to the corner) at which the above-mentioned difference is below 1 pixel (dist_1) and 2 pixels (dist_2) are given in Table 1. This table shows also the maximal difference ($\mathrm{dist}_{\max}$) which was measured for each lens.

Distortion has an influence on the true field of view. Knowing the positions of the stars in our recorded images, we were able to determine true fields of view and compare them to those given by the manufacturers.

4.2 Limiting magnitude and optical efficiency

The determination of limiting magnitudes for long and short exposures was made by eye by three persons independently and the results averaged. Limiting magnitudes, after correcting to the same size of aperture, translate into the optical efficiency.

4.3 Star images

An ideal lens would produce almost point-like images of stars across the whole FOV of the camera. Of course this was not the case for lenses tested by us. Aberrations such as coma, astigmatism, field curvature and chromatic aberration combine to produce stellar images which are blurry and elongated. To estimate this effect we measured the profiles (FWHM[2]) of about 100 star images per recorded long exposure frame. The mean values of FWHM derived for each lens are also shown in Table 1.

[2]Full width, half maximum. This describes the full width (i.e. edge to edge, not center to edge) at which the intensity has fallen to half the maximum.

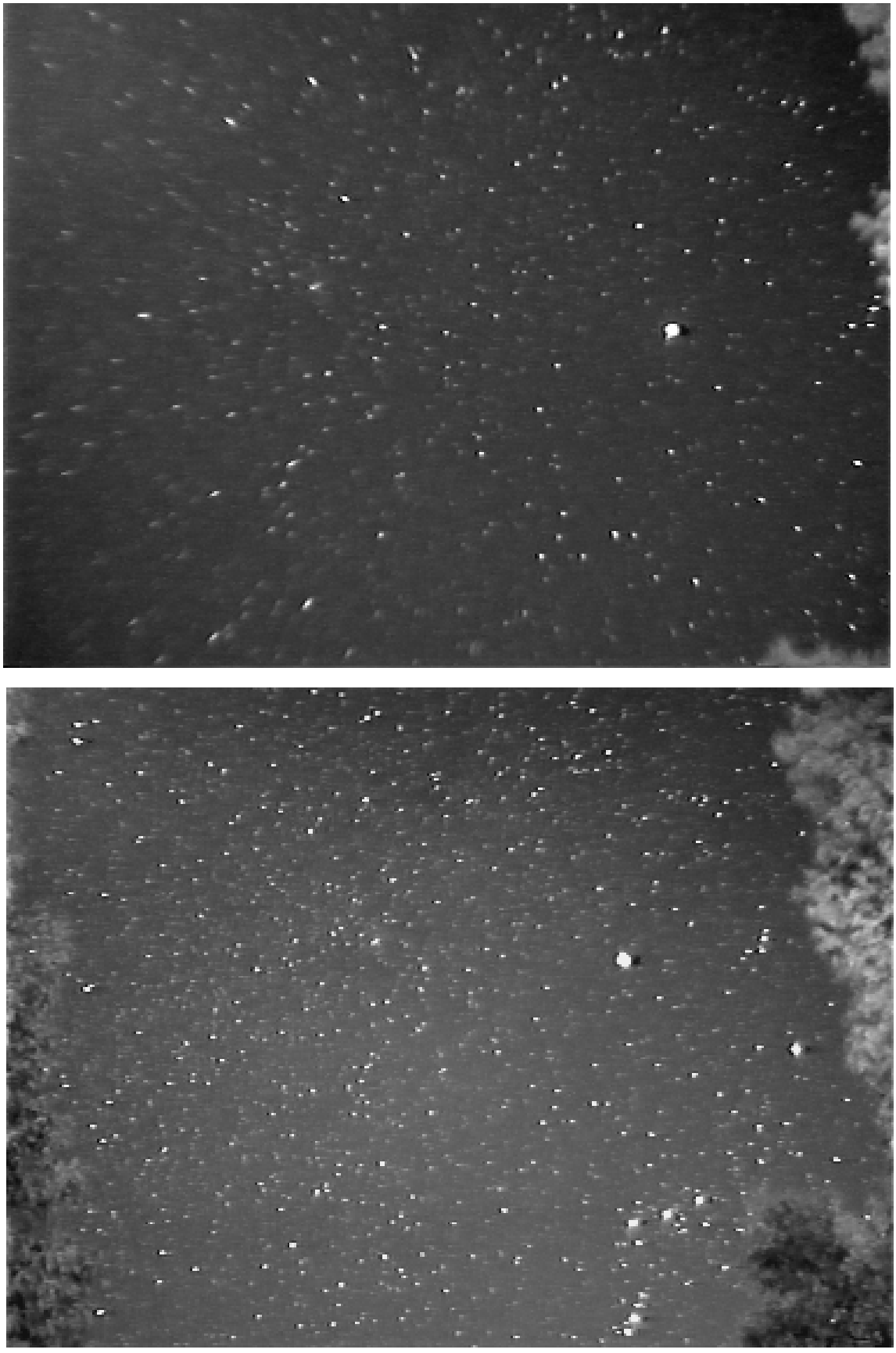

Figure 3 – Example of images for long exposures. Top: EVETAR $f/1.4$, $f = 12$ mm. The cheapest and the worst picture quality lens. Bottom: ERNITEC $f/1.2$, $f = 8$ mm. The most focused image. These images have been enlarged so that the pixels are visible, to allow a critical appraisal of the quality.

Figure 4 – Example of images for long exposures. Top: COMPUTAR $f/1.2$, $f = 4$ mm. The best lens in the tests. Bottom: COMPUTAR $f/0.8$, $f = 3.8$ mm. The fastest lens in the tests. These images have been enlarged so that the pixels are visible, to allow a critical appraisal of the quality.

Table 2 – Final results of the test, with results measured in points rather than physical units. (a): auto iris (adjusts automatically to light level); (z): zoom. F: focal ratio, i.e. f/d. FWHM: stellar image width. For an explanation of other quantities, see the Section 4.

Name	f (mm)	F	FWHM (0–10)	OE (0–10)	$\text{dist}_{\max}$ (0–3)	dist_1 (0–3)	dist_2 (0–6)	Total (0–32)
ERNITEC (a)	2.8	1.4	9	6	2.1	2.4	6.0	25.5
COMPUTAR	8.0	1.2	8	6	2.1	2.1	6.0	24.2
SIEMENS	12.0	1.2	8	4	2.7	3.0	6.0	23.7
COMPUTAR	4.0	1.2	10	10	0.3	0.9	2.4	23.6
ERNITEC	8.0	1.2	10	6	1.5	1.2	4.2	22.9
SIEMENS	4.0	1.2	9	6	0.3	1.8	4.8	21.9
PENTAX	8.0	1.2	5	5	2.4	2.7	6.0	21.1
SIEMENS	6.0	1.2	7	8	0.9	1.2	3.6	20.7
TAMRON (z)	2.8	1.4	8	7	0.3	0.6	1.8	17.7
EVETAR	12.0	1.4	3	3	2.7	3.0	6.0	17.7
TAMRON (z)	3.0	1.0	7	4	1.2	1.2	3.6	17.0
SIEMENS (a)	4.0	1.2	5	7	0.6	0.9	3.0	16.5
COMPUTAR (a)	3.8	0.8	1	1	1.2	1.5	4.2	8.9

4.4 Criteria

A summary of our tests is given in Tables 1 and 2. The categories which were taken into account to get the final mark were: mean FWHM (0–10 points), OE - optical efficency, (0–10 points), $\text{dist}_{\max}$ - maximal distortion (0–3 points), dist_1 - size of field of view with distortion below 1 pixel (0–3 points), dist_2 - size of field of view with distortion below 2 pixels (0–6 points). An ideal lens would get the total number of 32 points. The numbers of points collected by each lens in each category and the total scores are presented in Table 2.

5 Conclusions

The best lenses in our tests were those produced by Ernitec and Computar. Our work was performed in order to choose the best lenses to use on video cameras of the *Polish Fireball Network*. We were mostly interested in 4 and 8 mm lenses and thus we have naturally chosen Computars and Ernitecs.

The results for very fast lenses were a big surprise for us. These two lenses had the worst optical efficiency and poor FWHM. They were also the most expensive among the lenses tested. We suppose that the materials used for their construction comes from the early 1990s. Thus their quality of, for example, multilayer anti-reflection coatings could be much worse than in those lenses currently manufactured.

Full results of our tests will be available on the *PFN* web page at `http://pfn.pkim.org` .

Acknowledgements

This work was supported by a Siemens Building Technologies grant for the Polish Fireball Network.

References

Hecht E. (1998). *Optics*. Addison-Wesley, Reading, Mass., USA, 3rd edition.

Molau S. (1994). "MOVIE: Meteor Observation with VIdeo Equipment". In Roggemans P., editor, *Proc. IMC, Puimichel, France*, pages 71–75. International Meteor Organization, Potsdam.

Molau S. (1995). "MOVIE — analysis of video meteors". In Knoefel, A. & Roggemans P., editor, *Proc. IMC, Belogradchik, Bulgaria*, pages 51–61. International Meteor Organization, Potsdam.

Molau S. and Nitschke M. (1996). "Computer-based meteor search: a new dimension in video meteor observation". *WGN*, **24:4**, 119–123.

Molau S., Nitschke M., de Lignie M., Hawkes R. L., and Rendtel J. (1997). "Video observations of meteors: history, current status, and future prospects". *WGN*, **25:1**, 15–20.

Olech A., Wiśniewski M., Żołądek P., Krasnowski M., Fietkiewicz K., Kwinta M., Dorosz D., Lemiecha A., Lemiecha M., Sajdak M., Turek P., Kędzierski P., Mularczyk K., Złoczewski K., Kowalski T., Kowalski Ł., Fajfer T., Wójcicki K., Szary A., and Kozłowski S. (2005). *WGN*. in preparation.

Ray S. (1977). *The Lens and All its Jobs*. Focal Press, London.

Welford W. (1991). *Useful Optics*. Univ. Chicargo Press, Chicargo.

Wiśniewski M., Kędzierski P., Mularczyk K., and Złoczewski K. (2003). "Polish Automated Video Observations (PAVO)". *WGN*, **31:1**, 33–34.

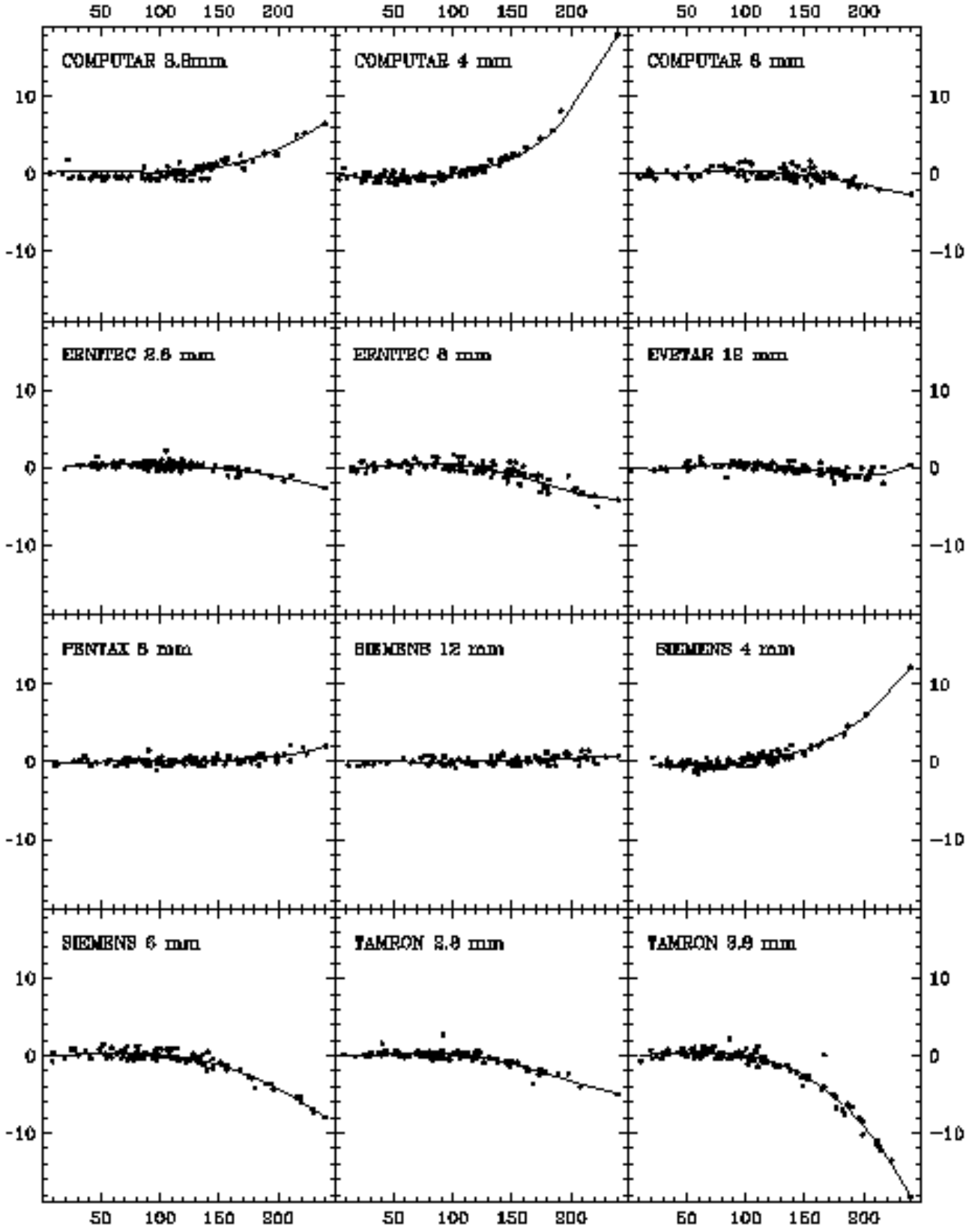

Figure 5 – Distortions of tested lenses as a function of distance from centre of view. Vertical axes: observed−correct positions, in pixels. Horizontal axes: distance from the center of the field of view, in pixels.

History

Meteor Beliefs Project: Meteors as symbols of love

Andrei Dorian Gheorghe [1], *Alastair McBeath* [2] *and Richard Taibi* [3]

Three items depicting meteoric love symbolism in Western ideas spanning from the 13th century AD to modern times are presented, with some discussion.

Received 2004 December 11

1 Introduction

A somewhat eclectic selection of items are presented below, which relate to meteors being seen as symbolic of love in one form or another. There is no attempt here to give a systematic overview of the topic, merely to show a few items of interest which have come readily to hand. Elements of this subject have already been touched upon in earlier Meteor Beliefs Project articles, and also (Gheorghe & McBeath, 1998) and (McBeath & Gheorghe, 1999) with some of the Romanian variants. Given the nature of the material, we decided February was an appropriate time to publish these thoughts, with February 14 being St Valentine's Day, patron saint of lovers (amongst other things).

2 Dante's *Paradiso*

The great Italian poet Dante Alighieri (1265–1321) is best remembered today for his superb epic, *The Divine Comedy*. Its three parts — 'Inferno', 'Purgatorio' and 'Paradiso' — describe in intricate detail his journey in a vision through the medieval Christian versions of Hell, Purgatory, and finally Paradise. It sets down the clearest single-text conception of the medieval cosmos that survives. Dante's journey passes down through the centre of the Earth, out the other side, and on beyond the Earth, through the layers of crystalline spheres believed to comprise the visible universe in his day. As always, we recommend anyone interested to read the full texts of what we merely extract from here.

Our selection comes from 'Paradiso' Canto XV, lines 10–27, a passage set in the crystal sphere of Mars, the Fifth Heaven. It is part of the opening to a section where Dante is to meet the soul of his 12th century ancestor, Cacciaguida. The text is cited here from (Sisson & Higgins, 1993, pp. 413–414):

> If, for the love of what does not endure,
> A man gives up that love eternally,
> He well deserves to suffer without end.
>
> As through a clear and tranquil starlit sky
> From time to time there runs a sudden fire,
> Moving eyes which were gazing steadily,
> And it seems as if a star is moving its station
> Until one sees that, from the place where it lit up,
> Nothing is lost, and that it does not last long;
>
> So from the right-hand tip of that cross
> To its foot a star appeared to run,
> From the constellation which shone there.
>
> Nor did the jewel come off its ribbon,
> But travelled along by way of the radial bands
> And seemed like a flame behind alabaster.
>
> So did Anchises's shade present himself,
> If we are to believe our greatest muse,
> When, in Elysium, he perceived his son.

The 'sudden fire' is obviously a meteor, being likened to love which is not eternal. In Dante's conception, this eternal love would be for his god. Clearly, Dante intended meteors to be symbolic of a more transitory, earthly, love.

Anchises in Greek myth was Aeneas' father (we met Aeneas earlier in relation to the meteoritic Palladium (McBeath& Gheorghe, 2004)). Aeneas was commonly depicted in Greek art carrying his aged, infirm, yet wise, father on his back away from Troy to safety. Later myths described how he travelled into the Underworld to meet his dead father's shade. Dante's specific reference is to the *Aeneid* of Virgil ('our greatest muse'), Book VI, line 684 and following. Anchises describes souls in very fiery, meteoric terms in *Aeneid* VI. 719–751 (Fairclough, 1935, pp. 556–559).

3 Millet's *The Shooting Stars*

Jean-François Millet (1814–1875) was a French painter, whose early work included a series of female nude figures. Part of this material was 'The Shooting Stars' of 1847–49, a 19×35 cm oil on board painting.

The background of the painting is a dark night-blue, with a few pale dots as stars. Across this sky-scape, sweeping up from bottom right towards the top left, are two young, well-formed, male-female couples, drawn as if flying without wings through the air. In each pairing, the male is naked, the female has at least part of her lower body and limbs covered by a long, thin, transparent, flowing garment. In both cases, this garment gives the impression of a pale flowing 'tail' to the couple, although both 'tails' and the lower legs of the more distant couple, pass off the right edge of the image. All four figures have dark hair, the males' shorter than the

[1]Bd. Tineretului 53, bl. 65, ap. 40, sect. 4, Bucureşti, Romania. Email: sarm@romwest.ro
[2]12a Prior's Walk, Morpeth, Northumberland, NE61 2RF, England, UK. Email: meteor@popastro.com
[3]7002 Coolridge Drive, Temple Hills, MD 20748, USA. Email: rjtaibi@hotmail.com

females', as far as this can be judged. The two women are pale, almost silvery white in colour, and there is nothing except traces of form and shadow to tell where their garments begin and their bodies end. The two men have a darker skin, chiefly grey in colour.

The nearer pair are shown somewhat ahead of the farther, along a similar line through the sky. This couple has both characters facing forwards, the male posed as if towing the female through water, with his hands beneath her armpits, while his legs partly wrap around the sides of her upper torso. Her arms are languorously flung wide because of this passively captive pose, and she lies with her head reclining against his chest, eyes closed as if in sleep or ecstasy. He is gazing up towards the top left corner. An orange-red glow outlines much of his body, and part of hers, mostly where they meet the background blue of the sky. The glow appears more to be coming from the male figure than a reflection of some unseen light source, and given the picture's title, it is probably intended to suggest the glow of a meteor passing across the sky. Part of the background seems to have a pale red colour patchily streaked across it too, which may be intended to signify the realm of fire, long believed part of the upper air near where meteors ignited. Behind these figures, is a dark, shadowy, flowing garment, which might be attached to the male's unseen waist, or the female's hidden shoulders, like a cloak. It too passes off the bottom right corner of the board.

The farther couple has the woman shown in side view, again with her eyes closed, and head tilted back, this time against the man's right shoulder. Her left arm reaches up so her hand rests on his upper right arm. This male is in three-quarter rear-view, his form partly hidden by the foreground couple, and he seems to have much less of a red glow about him than the closer male. Both his legs are crossed beneath the woman's, his right arm across her stomach and thigh, as previously, rather as if he is holding her to tow her through water.

The painting has been suggested as showing the doomed souls of Paolo Malatesta and Francesca da Rimini, adulterous lovers who were killed sometime between 1283–86, and who featured in Dante's 'Inferno' (Canto V) in the Second Circle of Hell, perpetually cast about in the air by stormy winds, never able to rest. (See Sisson & Higgins, 1993, pp. 65–69, and pp. 513–514 for historical notes on this couple.) As the painting's title does not say so, there is no way to be sure, as there are no supporting records for this identification from the painter himself. Other authors have been more general in their comments, indicating only that the personified meteors soaring through the air perhaps show the transcendental nature of erotic love. Olson (1985, p. 87) goes further:

'During the nineteenth century, eroticism and comets could go hand in hand. Comets and their cousins, meteors or shooting stars, were discreet allusions to adultery (*The Scarlet Letter*) and to transcendental love (*War and Peace*), and even simply to the very act of physical love, as in the socialist Jean-François Millet's painting *The Shooting Stars*'.

The Scarlet Letter was a novel by Nathaniel Hawthorne; *War and Peace* Leo Tolstoy's great Napoleonic Wars epic.

Olson continues: 'Millet's figures themselves emit light, and the red contours around the man of the left-hand couple communicate the heat of passion, while the elongation of the figures formally conveys their longing voluptuousness, transient as shooting stars.'

She also shows the painting as Figure 78, p. 86, while the painting itself still hangs in the National Museum & Gallery of Wales in Cardiff[1].

4 *Stars Fell on Alabama*

Skipping forward another 150+ years, and crossing the Atlantic Ocean to America, our last curiosity comes from a modern car license plate from Alabama. The state has printed a logo on its vehicle registration tags that reads, 'Stars fell on Alabama'. A check on the Internet confirmed that the logo referred to the Leonid storm that was seen in Alabama and the eastern half of North America before dawn on November 13, 1833.

Local Alabama newspaper accounts of the awesome spectacle perpetuated the public's memory of the event. Then a century after the storm, in 1934, a book describing the meteor storm and other Alabamian events was published in the state by Carl Carmer, with the title 'Stars Fell on Alabama'. Some years later, two song writers, Mitchell Parish and Frank Perkins, used the phrase as a love song title. Undoubtedly the song further ingrained the phrase in the public's consciousness. In 2002, the state made the phrase, now a reference to the song, part of the state's character by imprinting it on the license plates. Now, the tag provokes curiosity about the phrase, and the local Chamber of Commerce hopes it will also prompt non-residents to visit Alabama.

Of course, it is the song we are particularly interested in here. Its chorus runs:

> I never planned in my imagination,
> a situation so heavenly
> A fairy land that no one else could enter
> And in the center, just you and me, dear
> My heart beat like a hammer, my arms wound
> around you tight
> And stars fell on Alabama last night.

The 'falling stars' are again a metaphor for rising passion, and in the song's description, it is easy to see a link back to the clasping, entwined couples of Millet's painting of 1847–49.

5 Conclusion

These few items show some of the love symbolism associated with meteors in Western thought at least. There are undoubtedly more such to be found, and we may return to this topic at a later date. As ever, if you have come across something on this or other subjects you

[1]The painting can be seen online via `www.nmgw.ac.uk/art/collections/db/` ; search under 'Artists' for Millet.

think might be useful to the Meteor Beliefs Project, do please get in touch with us.

References

Fairclough H. R. (1935). *Virgil Volume I: Eclogues, Georgics, Aeneid I–VI (revised edition).* William Heinemann & Harvard University Press (Loeb Classical Library imprint), (1967 reprint).

Gheorghe A. D. and McBeath A. (1998). "Romanian meteor mythology". In Knöfel A. and McBeath A., editors, *Proceedings of IMC 1997, Petnica, Yugoslavia*, pages 82–88. IMO.

McBeath A. and Gheorghe A. D. (1999). "Luceafărul: A Romanian meteor-inspired poem". *WGN*, **27:5**, 255–258.

McBeath A. and Gheorghe A. D. (2004). "Meteor Beliefs Project: The Palladium in ancient and early medieval sources". *WGN*, **32:4**, 117–121.

Olson R. J. M. (1985). *Fire and Ice: A History of Comets in Art.* National Air and Space Museum, Smithsonian Museum & Walker and Co.

Sisson C. H. and Higgins D. H. (1993). *Dante Alighieri: The Divine Comedy (updated version).* 'The World's Classics' imprint. Oxford University Press.

The International Meteor Organization

web site http://www.imo.net

Council

President: Jürgen Rendtel,
Eschenweg 16, D-14476 Marquardt, Germany.
tel. +49 33208 50753
e-mail: jrendtel@aip.de
Vice-President Alastair McBeath
12A Prior's Walk, Morpeth,
Northumberland NE61 2RF, UK.
tel. +44 1670 518487
e-mail: meteor@popastro.com
Secretary-General: Robert Lunsford
161 Vance Street, Chula Vista,
CA 91910-4828, USA. tel. +1 619 585 9642
e-mail: lunro.imo.usa@cox.net
Treasurer: Ina Rendtel
Mehlbeerenweg 5, D-14469 Potsdam, Germany
tel. +49 331 520 707
e-mail: IRendtel@t-online.de
Postal (giro) account number: 5472 34-107
Bank code: 100 100 10 Postbank Berlin
When paying, state bank code and postbank as well as account number!
BIC: PBNKDEFF
IBAN: DE86 1001 0010 0547 2341 07.

Other council members:
Rainer Arlt, Friedenstraße 5, D-14109 Berlin, Germany. e-mail: rarlt@aip.de
David Asher, Armagh Observatory, College Hill, Armagh BT61 9DG, Northern Ireland, UK.
e-mail: dja@star.arm.ac.uk
Malcolm Currie, 25, Collett Way, Grove, Wantage, Oxfordshire OX12 0NT, UK.
e-mail: mjc@star.rl.ac.uk
Marc Gyssens, Heerbaan 74, B-2530 Boechout, Belgium. e-mail: marc.gyssens@luc.ac.be
André Knöfel, Habichstraße 1,
D-15526 Reichenwalde, Germany.
e-mail: aknoefel@minorplanets.de
Sirko Molau, Abendstalstraße 13b,
D-84072 Seysdorf, Germany.
e-mail: sirko@molau.de
Mihaela Triglav-Čekada, Streliška 9,
SI–1000 Ljubljana, Slovenia.
e-mail: mtriglav@yahoo.com

Commission Directors

FIreball DAta Center: André Knöfel
Photographic Commission: Marc de Lignie
Steve Bikostraat 298,
NL-3573 BH Utrecht, The Netherlands
e-mail: m.c.delignie@xs4all.nl
Radio Commission: vacant
Telescopic Commission: Malcolm Currie
Video Commission: Sirko Molau
Visual Commission: Rainer Arlt

WGN

Editor: Chris Trayner
32 Moor Park Villas, Leeds LS6 4BZ, UK
fax: +44 113 3432032; mark "for C. Trayner"
tel: +44 113 2302687 e-mail: wgn@imo.net ;
include METEOR in the e-mail subject line
Editorial board: R. Arlt, M. Gyssens, A. McBeath, J. Rendtel, M. Triglav-Čekada.
Advisory board: D.J. Asher, M. Beech, P. Brown, M. Currie, M. de Lignie, W.G. Elford, R.L. Hawkes, D.W. Hughes, J. Jones, C. Keay, G.W. Kronk, R.H. McNaught, P. Pravec, G. Spalding, M. Šimek, I. Williams.

IMO Sales

Available from the Treasurer	€	$
Proceedings of the International Meteor Conference		
1990–1996	5	5
1997	Out of print	
1998–2000, 2002–2003	6	6
2001 — on CD only	5	5
2004	8	8
Back issues of WGN		
Vols. 19–22 (1991–1994) per complete volume	10	10
Vols. 23–29 (1995–2001) per complete volume	18	18
Vol. 30 (2002) per complete volume	20	20
WGN Observational Report Series		
Vols. 1–5 (1988–1992), 7–8 (1994–1995) Visual Observations, per volume	8	8
Vol. 6 (1993) Visual Observations and Electrophonic Fireball Catalogue	8	8
Vols. 9–14 (1996–2002) Visual Observations, per volume	10	10
Other publications		
Photographic Meteor Database (1986)	4	4
Photographic Astrometry + diskette	7	7

Meteor imaging past and present

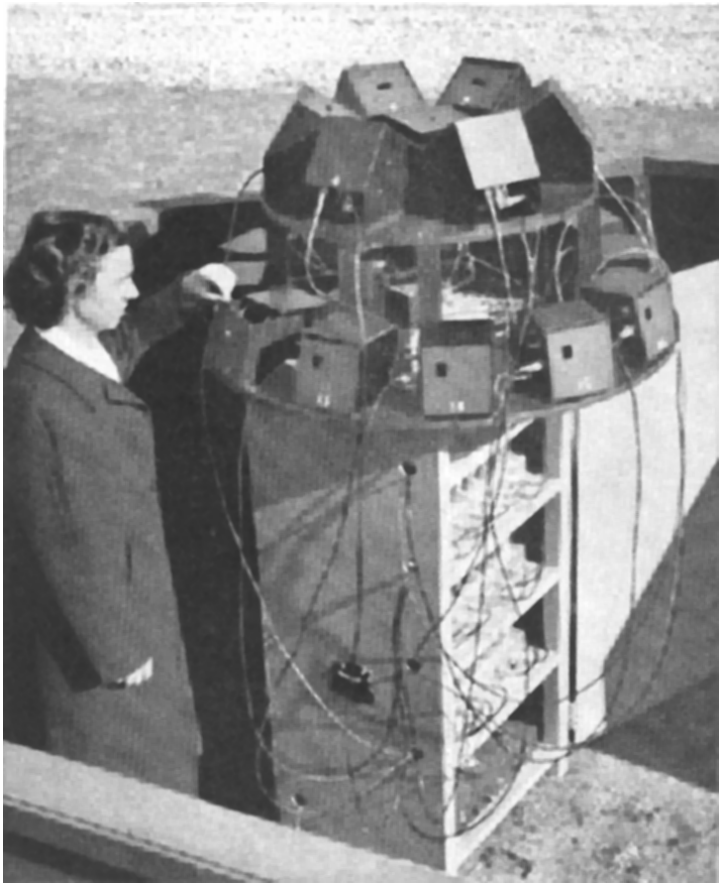

An 1949 Canadian meteor detector with 19 photomultiplier tubes, each covering 30°×36° of the sky without lenses. This 19-pixel all-sky real-time camera was decades ahead of its time. *From* Meteor Science and Engineering, by D.W.R. McKinley, McGraw-Hill, New York (1961), pp. 62–63. Reproduced by kind permission of the publishers.

Robert Haas (Dutch Meteor Society) with an array of cameras use for the Leonid compaigns 1998–2001: the 'Hazen' array.

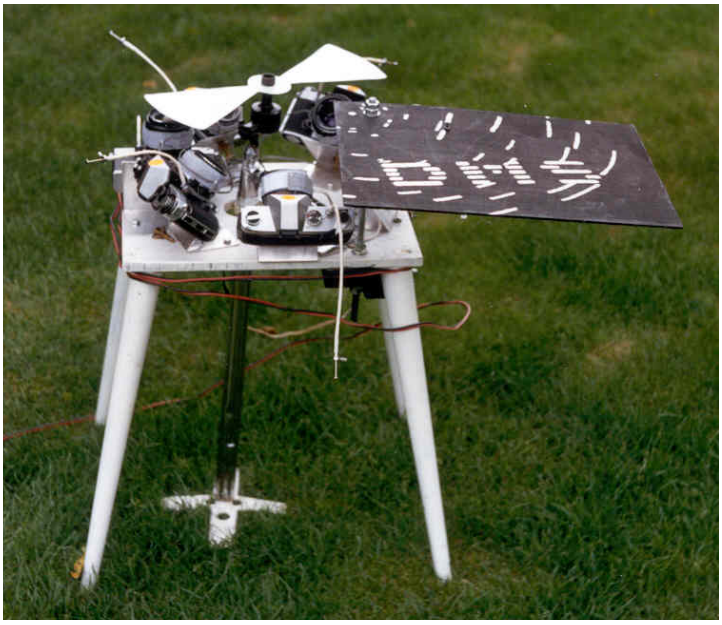

An earlier meteor camara array used by the Dutch Meteor Society.

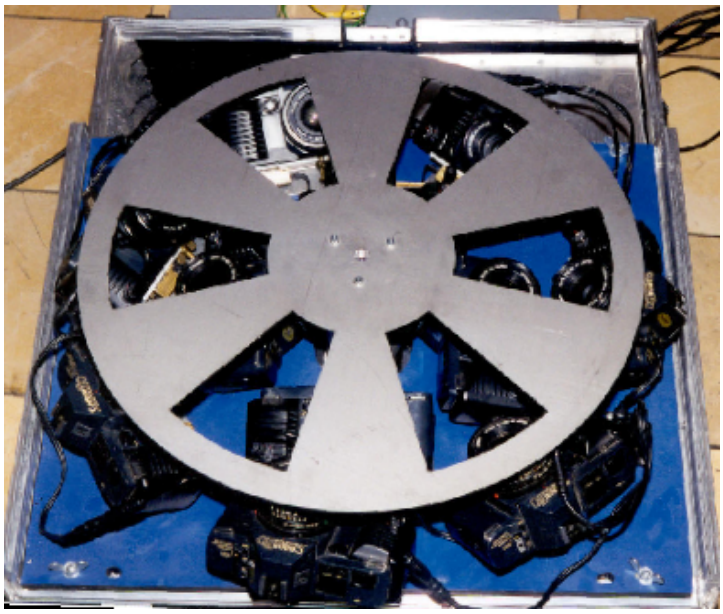

Detail of more equipment of the 'Hazen' array.